

Space Science Reviews manuscript No.
 (will be inserted by the editor)

Strong gravitational lensing and microlensing of supernovae

Sherry H. Suyu^{1,2,3} · Ariel Goobar⁴ ·
 Thomas Collett⁵ · Anupreeta More^{6,7} ·
 Giorgos Vernardos⁸

Draft: January 20, 2023 / Received: date / Accepted: date

Abstract Strong gravitational lensing and microlensing of supernovae (SNe) are emerging as a new probe of cosmology and astrophysics in recent years. We provide an overview of this nascent research field, starting with a summary of the first discoveries of strongly lensed SNe. We describe the use of the time delays between multiple SN images as a way to measure cosmological distances and thus constrain cosmological parameters, particularly the Hubble constant, whose value is currently under heated debates. New methods for measuring the time delays in lensed SNe have been developed, and the sample of lensed SNe from the upcoming Rubin Observatory Legacy Survey of Space and Time (LSST) is expected to

Sherry H. Suyu
 E-mail: suyu@mpa-garching.mpg.de

Ariel Goobar
 E-mail: ariel@fysik.su.se

Thomas Collett
 E-mail: thomas.collett@port.ac.uk

Anupreeta More
 E-mail: anupreeta@iucaa.in

Giorgos Vernardos
 E-mail: georgios.vernardos@epfl.ch

¹Technical University of Munich, TUM School of Natural Sciences, Department of Physics, James-Franck-Straße 1, 85748 Garching, Germany

²Max-Planck-Institut für Astrophysik, Karl-Schwarzschild-Str. 1, 85748 Garching, Germany

³Institute of Astronomy and Astrophysics, Academia Sinica, 11F of ASMB, No.1, Section 4, Roosevelt Road, Taipei 10617, Taiwan

⁴The Oskar Klein Centre, Department of Physics, Stockholm University, Albanova University Center, SE-106 91 Stockholm, Sweden

⁵Institute of Cosmology and Gravitation, University of Portsmouth, Dennis Sciama Building, Burnaby Road, Portsmouth, PO1 3FX, UK

⁶The Inter-University Centre for Astronomy and Astrophysics (IUCAA), Post Bag 4, Ganeshkhind, Pune 411007, India

⁷Kavli Institute for the Physics and Mathematics of the Universe (IPMU), 5-1-5 Kashiwanoha, Kashiwa-shi, Chiba 277-8583, Japan

⁸Institute of Physics, Laboratory of Astrophysics, Ecole Polytechnique Fédérale de Lausanne (EPFL), Observatoire de Sauverny, 1290 Versoix, Switzerland

provide competitive cosmological constraints. Lensed SNe are also powerful astrophysical probes. We review the usage of lensed SNe to constrain SN progenitors, acquire high- z SN spectra through lensing magnifications, infer SN sizes via microlensing, and measure properties of dust in galaxies. The current challenge in the field is the rarity and difficulty in finding lensed SNe. We describe various methods and ongoing efforts to find these spectacular explosions, forecast the properties of the expected sample of lensed SNe from upcoming surveys particularly the LSST, and summarize the observational follow-up requirements to enable the various scientific studies. We anticipate the upcoming years to be exciting with a boom in lensed SN discoveries.

Keywords gravitational lensing: strong · Gravitational lensing: micro · supernovae: general · (Cosmology:) distance scale · (Cosmology:) cosmological parameters · (ISM:) dust, extinction

Contents

1	Brief history	2
2	Cosmological probe	6
3	Astrophysical probe	16
4	Searches and Rates	22
5	Summary	28

1 Brief history

In an insightful and pioneering publication, Refsdal (1964) pointed out that supernovae (SNe) would be particularly interesting sources for studies involving strong gravitational lensing. This was arguably among the biggest early milestones in the field of gravitational lensing, following the realisation by Zwicky (1937) that the scenario, first proposed by Einstein in 1936, had realistic applications in extragalactic astronomy. Refsdal pointed out that the measurement of the time delay between the arrival of SN images could be used to infer the Hubble constant (H_0).

1.1 History of searches for lensed SNe behind clusters

The idea to use “gravitational telescopes”, i.e., known lensing galaxy clusters, to boost the faint signals from distant supernovae started to get traction about thirty years ago (Kovner and Paczynski, 1988; Sullivan et al., 2000; Gunnarsson and Goobar, 2003). Since the lensing magnification boosts the signal from the faint distant source behind the lens by a factor of μ , but leaves the dominant foreground sky noise unaffected, the signal-to-noise ratio scales as $SNR \propto \mu\sqrt{t}$, hence leading to a gain factor μ^2 in exposure length. However, the solid angle at the source planes shrinks by a factor μ behind the lens. Thus, the net gain/loss of searching for supernovae behind massive clusters is therefore a non-trivial combination of field of view, limiting depth, and supernova luminosity functions. Although not spectroscopically confirmed, several SN candidates were eventually found in cadenced observations in the Near-IR at the Very Large Telescopes (VLT) of the European

Southern Observatory (ESO) (Stanishev et al., 2009; Goobar et al., 2009), including a $z = 1.7$ core-collapse SN behind Abell 1689, with a lens model inferred magnification $\mu = 4.3 \pm 0.3$ (Amanullah et al., 2011). In spite of the limitations of the survey, Petrushevska et al. (2016) demonstrated the power of gravitational lensing to place meaningful limits on the rate of core-collapse supernovae at very high redshifts.

1.2 Discoveries!

PS1-10afx was first reported by Chornock et al. (2013) as an unusual superluminous SN. However, shortly thereafter, Quimby et al. (2013) showed that it was a perfect match to a lensed SN Ia at redshift $z = 1.388$, with a large amplification, $\mu \sim 30$. Quimby et al. (2014) eventually also identified a foreground lens, at $z = 1.117$. Even if the putative lensing object was too close to the SN, it was consistent with lensing models and existing data. Since the lensed SN Ia classification only gained acceptance four years after the explosion, further investigation of the lensing nature of the SN or its type was not possible. Moreover, a subsequent single-band HST imaging (PI: Chornock) proved insufficient to verify the presence of any lensed images of the SN host galaxy.

The first detection of multiple images from a supernova came with SN Refsdal at redshift $z = 1.49$ (Kelly et al., 2015), found in Hubble Space Telescope (HST) surveys of the massive lensing galaxy cluster MACS J1149.6+2223 at $z = 0.54$. Based on both light curve shapes and spectroscopy, SN Refsdal was classified as a Type II SN, resembling the iconic SN 1987A in the LMC (Kelly et al., 2016b). This is a peculiar class of faint SNe, quite rare in the local universe. At the time of discovery, 4 multiple images of the SN were visible with HST (images S1-S4, see Fig. 1 taken from Grillo et al. 2018), in a cross configuration around one of the foreground cluster galaxies. There are two other images of the background spiral galaxy hosting the SN, labelled as SX (inset (a) in Fig. 1) and SY (the northern-most image, just outside the top-right corner of inset (a)).

Using mass models of the cluster, the discovery team (Kelly et al., 2015) predicted that SY happened before S1-S4, whereas SX would appear after S1-S4. However, the time of SX reappearance was uncertain from their model, ranging from 1 to 10 years. To refine the delay prediction, Grillo et al. (2016) used the Multi Unit Spectroscopic Explorer (MUSE; Bacon et al., 2010) on ESO’s VLT to obtain spectroscopic observations of the field. The spectroscopic redshift measurements helped to separate foreground lenses from background sources. This spectroscopic data set was shared with multiple modelling teams, who attempted to predict the reappearance of image SX using the new observational data. Teams predicted their delays before the reappearance (Treu et al., 2016; Jauzac et al., 2016; Grillo et al., 2016; Kawamata et al., 2016), providing a true blind test of the predictions and the modelling capabilities. Most teams predicted a short time delay of SX with respect to S1, within a year’s time. Kelly et al. (2016a) detected the reappearance of SX in December 2015, and the resulting constraint on the time delay and magnification of SX agreed well with the predictions from two teams (Grillo et al., 2016; Kawamata et al., 2016).

Through the monitoring of the multiple images of SN Refsdal, Rodney et al. (2016) have measured the time delays and magnification ratios among images S1,

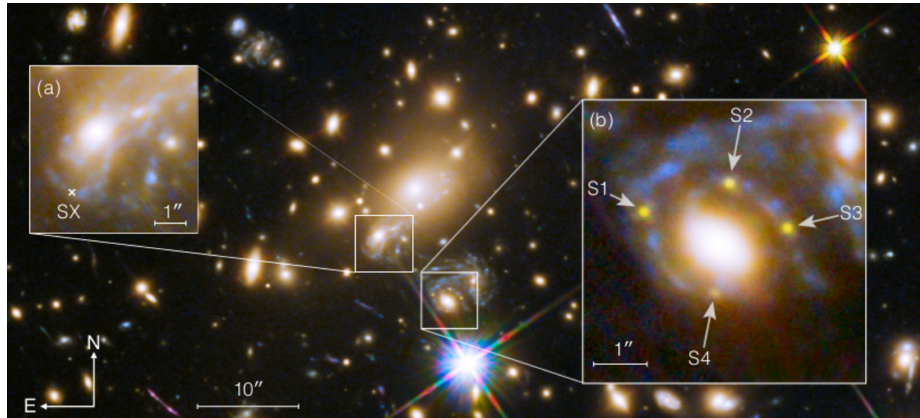


Fig. 1 Hubble Space Telescope image of SN Refsdal, the first strongly lensed SN system with spatially resolved images. Inset (a) shows the image SX that was detected in December 2015 (Kelly et al., 2016a), and inset (b) shows the multiple images S1, S2, S3 and S4 that were first discovered in November 2014 (Kelly et al., 2015). There is another image SY located in the northern most image of the spiral host galaxy, next to the top-right corner of the inset (a). Image taken from Grillo et al. (2018). Original image credit: NASA, ESA/Hubble.

S2, S3 and S4. The detection of the reappearance of image SX provided an estimate of its time delay with respect to the other images (Kelly et al., 2016a), and the time-delay measurement from subsequent monitoring is forthcoming (P. Kelly, private communications). The SX time delay is expected to be precise with uncertainties of at most a few percent given its long delay of ~ 1 year, providing a great opportunity of measuring the Hubble constant with gravitational lens time delays (e.g., Grillo et al., 2018, 2020, Kelly et al. in prep.).

The first spatially resolved multiply-imaged Type Ia supernova, iPTF16geu, was detected by the intermediate Palomar Transient Factory (Goobar et al., 2017). As shown in Fig. 2, the ground-based imager at iPTF could not spatially resolve the very compact system with Einstein radius $\theta_E = 0.3''$. However, because of the “standard candle” nature of SNe Ia, it became clear that strong lensing was the most likely explanation, since the SN was more than 30 standard deviations brighter than the expectations for a SN Ia at its measured redshift, $z = 0.409$. The spectra used to classify the supernova showed spectral lines from both the host galaxy at the same redshift, but also the deflecting galaxy at $z = 0.216$. Thanks to multi-band follow-up with HST, an accurate (model independent) measurement of the magnification was made, $\mu = 67.8^{+2.6}_{-2.9}$ (Dhawan et al., 2020), after correction for non-negligible extinction by dust in both the host and lens galaxies. The time delays between the SN images for this system were very small, about a day or less (More et al., 2017; Dhawan et al., 2020). The flux ratios between the supernova images (see Fig. 2) were not consistent with expectations from lensing, hinting contributions from stellar microlensing (More et al., 2017). This was further confirmed after differential dust extinction from within the lensing galaxy was also accounted for (Mörtsell et al., 2020).

In 2021, another strongly lensed SN, SN Requiem, was discovered in archival HST imaging of the galaxy cluster MACSJ0138.0–2155 by Rodney et al. (2021). A bright quiescent and evolved elliptical galaxy at redshift $z = 1.95$ is lensed

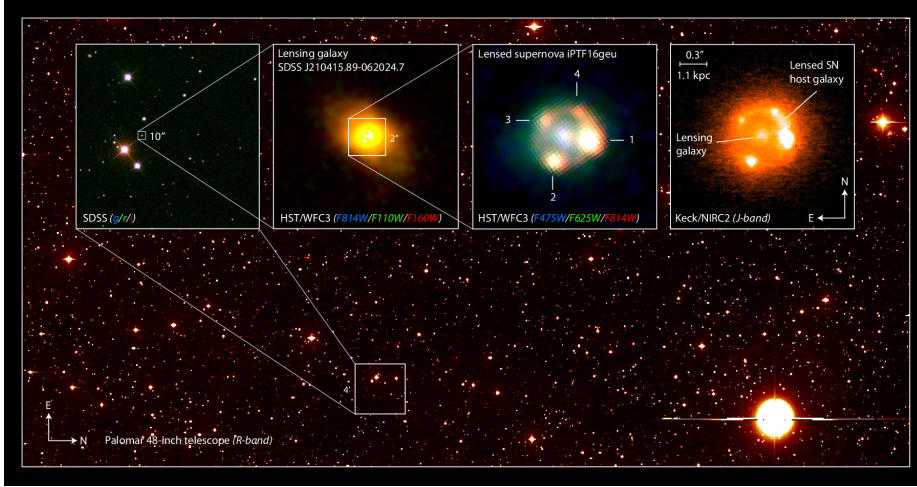


Fig. 2 Wide-field image from iPTF showing the portion of the CCD camera where iPTF16geu was found in modest seeing ($2''$). The insets show how the strong lensing nature, a quadruple lens with an Einstein radius of only $0.3''$, could be verified using HST imaging in the optical, and laser-guide-star adaptive-optics imaging from Keck in the Near-IR. Image credit: J. Johansson.

into giant arcs by the galaxy cluster, making this system one of the brightest NIR objects (e.g., Newman et al., 2018). Near the giant arcs are three point sources that were present in the single-epoch image in 2016 (Newman et al., 2018), but absent in the 2019 HST image (HST Program - REQUIEM; HST-GO-15663; PI:Akhshik). These 3 point sources are identified as multiple images of a SN hosted in the $z = 1.95$ galaxy, and the SN is likely to be of Type Ia. Based on the differences in the colour of the 3 SN images and SN Ia templates, the time delays could be estimated from the single-epoch observation in 2016, although with large uncertainties. The predicted time delays suggest that the fourth image of SN Requiem will appear in the future (circa 2037).

Recently, Goobar et al. (2022) discovered another strongly lensed SNe Ia, named Supernova Zwicky (a.k.a. SN 2022qmx), in the Zwicky Transient Facility (ZTF; Bellm et al., 2019). The discovery of this system is similar to the case of iPTF16geu – the multiple lensed SN Ia images are closely separated (with an Einstein radius of $\theta_E \sim 0.17''$) and not spatially resolved by ZTF, thus resulting in a brightness through lensing magnification that is substantially higher than expected for a SN Ia. Pierel et al. (2022) obtained HST imaging of this system, showing clearly the four multiple images of the SN Ia in a symmetric configuration. Based on the single-epoch photometry of the SN Ia images, Pierel et al. (2022) measured short time delays of < 1 day between the multiple images, which are consistent with the predictions from their multiple lens mass models obtained using different lensing software. Both Goobar et al. (2022) and Pierel et al. (2022) find anomalous flux ratios of the SN images compared to the smooth mass model predictions, indicating the presence of dust, millilensing and/or microlensing.

The fifth system of spatially-resolved lensed SN is reported very recently by Chen et al. (2022). A SN was lensed by one of the galaxies in the galaxy cluster Abell 370 in 2010 into three multiple images, and Chen et al. (2022) discovered

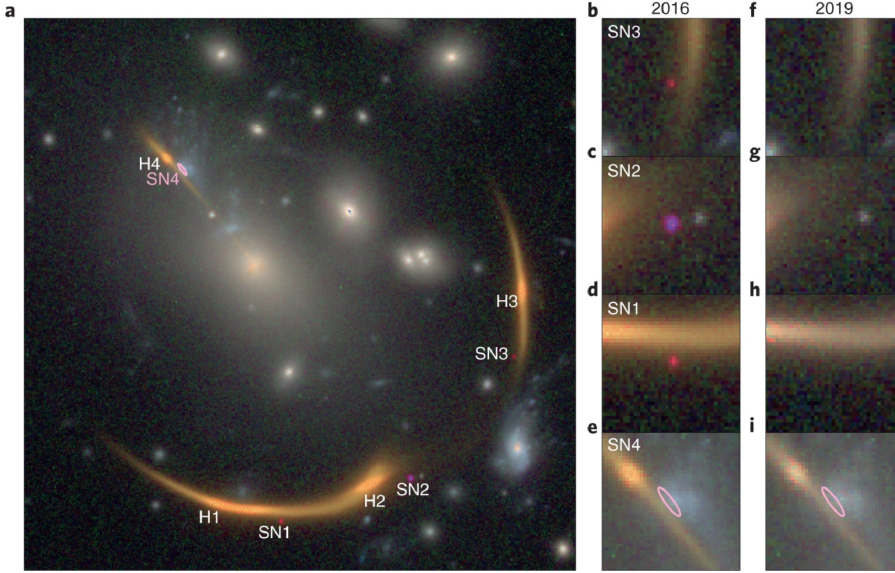


Fig. 3 Panel a): Color image of SN Requiem showing arc-like images of the distant host galaxy (H1-H4), the three SN images (SN1-SN3) and an ellipse pointing out the expected location of SN4. Panels b-i): zoomed-in regions around the SN locations from the data taken in 2016 (b-e) and 2019 (f-i). Figure taken from Rodney et al. (2021).

it in archival HST image, similar to the way that SN Refsdal was found. Based on their cluster lens mass modeling, Chen et al. (2022) estimated the rest-frame age of the SN for each of the three SN images, with the youngest one being a mere ~ 6 hours after explosion. Using the early-phase light curve obtained in the single-epoch HST observations with multiple filters, Chen et al. (2022) classified the SN as a core-collapse SN and measured its pre-explosion radius of $\sim 500M_{\odot}$, consistent with a red supergiant. The estimated photometric redshift of the SN host galaxy is ~ 3 .

These first few strongly lensed SNe have opened a new window to probe cosmology and supernovae through these spectacular phenomena. Two reviews (Oguri, 2019; Liao et al., 2022) on gravitationally lensed transients have illustrated the exciting utilities of lensed transients. Compared to these two reviews, we focus and dive deeper into the specific case of strongly lensed supernovae. In Section 2, we review the potential of lensed SNe as a cosmological probe. In Section 3, we describe the use of lensed SNe as an astrophysical probe, such as constraining the SN progenitors and dust in galaxies. In Section 4, we present various searches of lensed SNe and the expected rates in current and upcoming surveys. We summarise in Section 5.

2 Cosmological probe

While the idea of using lensed SNe for measuring the Hubble constant dates back to Refsdal (1964), this time-delay method was first realised with lensed quasars that

were discovered decades before lensed SNe, starting with the first lensed quasar system found by Walsh et al. (1979). The use of lensed quasars as a cosmological probe is reviewed by Birrer et al. (2022) in the same series (see also, e.g., Treu and Marshall, 2016; Suyu et al., 2018; Treu et al., 2022). We briefly summarise the approach of time-delay cosmography in Section 2.1, and focus on SNe as lensed background sources, which are “standardisable candles” and a relative distance indicator. In Section 2.2, we describe approaches to measure time delays of lensed SNe, particularly novel ones through spectroscopic observations of SNe, which complement conventional techniques using photometric light curves. In Section 2.3, we show the present cosmological constraints and future forecasts from lensed SNe.

2.1 Jackpot: two cosmological probes in one

We describe the various distance measurements that we can obtain from strongly lensed SNe, through the lensing time delays and the SN light curves. We briefly summarise the determination of the lensing distances that are covered in detail in the parallel reviews by, e.g., Birrer et al. (2022), and focus particularly on the new aspects that SNe bring.

The expression for the time delay between images i and j of a lensed SN is

$$\Delta t_{ij} = \frac{D_{\Delta t}}{c} \Delta \tau_{ij}, \quad (1)$$

where $D_{\Delta t}$ is the time-delay distance, c is the speed of light, and τ is the Fermat potential. The time-delay distance (e.g., Refsdal, 1964; Suyu et al., 2010) is defined by

$$D_{\Delta t} \equiv (1 + z_d) \frac{D_d D_s}{D_{ds}}, \quad (2)$$

where z_d is the deflector (lens) redshift, and D_d , D_s , and D_{ds} are the angular diameter distance to the deflector, to the source, and between the deflector and the source, respectively. The Fermat potential difference between two SN image positions $\boldsymbol{\theta}_i$ and $\boldsymbol{\theta}_j$ (with corresponding source position $\boldsymbol{\beta}$) is

$$\Delta \tau_{ij} = \tau(\boldsymbol{\theta}_i; \boldsymbol{\beta}) - \tau(\boldsymbol{\theta}_j; \boldsymbol{\beta}), \quad (3)$$

where the Fermat potential is

$$\tau(\boldsymbol{\theta}; \boldsymbol{\beta}) = \frac{1}{2} (\boldsymbol{\theta} - \boldsymbol{\beta})^2 - \psi(\boldsymbol{\theta}), \quad (4)$$

and $\psi(\boldsymbol{\theta})$ is the lens potential. The dimensionless surface mass density $\kappa(\boldsymbol{\theta})$, a.k.a. lensing convergence, is related to the lens potential via the Poisson equation,

$$2\kappa(\boldsymbol{\theta}) = \nabla^2 \psi(\boldsymbol{\theta}) \quad (5)$$

From Equation (1), we see that by measuring the time delays Δt_{ij} and modelling the deflection and line-of-sight mass distributions to get $\Delta \tau_{ij}$, we can infer the time-delay distance $D_{\Delta t}$. Since $D_{\Delta t}$ is a combination of three angular diameter distances (Equation 2) and is thus proportional to H_0^{-1} , time-delay lenses allow us to measure directly H_0 with weak dependence on other cosmological parameters.

When the lens galaxy stellar velocity dispersion is measured, then the combination of time delays, velocity dispersion and high-resolution imaging of the lens system allows D_d to be measured (e.g., Paraficz and Hjorth, 2009; Jee et al., 2015, 2019), in addition to $D_{\Delta t}$. The joint constraint of $D_{\Delta t}$ and D_d provides even more leverage on determining cosmological parameters (e.g., Jee et al., 2016; Yıldırım et al., 2020).

It is clear from Equation (4) that in order to constrain H_0 with strong lens time delays, one needs to know both the 2D lens potential and the unlensed source position, neither of which are directly observable. The use of lens modelling is required to infer these quantities. However, strong lens models are subject to degeneracies, which are a major source of uncertainty for time-delay cosmography (Schneider and Sluse, 2014). The largest problem is the mass-sheet degeneracy: re-scaling any model of the lensing convergence κ and adding a constant sheet of surface mass density leaves the predicted images unchanged, but alters the predicted time delay between the images (Falco et al., 1985). Breaking the mass-sheet degeneracy is therefore necessary to constrain H_0 from any lens with observations of image positions and time delays. In order to break the mass-sheet degeneracy, additional information is required, either non-lensing information (e.g., the dynamical mass of the system), the presence of sources at multiple redshifts (though see Schneider, 2014) or knowledge of the intrinsic luminosity or size of the unlensed source (Kolatt and Bartelmann, 1998). It is on this final point – a known luminosity of the source – that strongly lensed SNe shine as a powerful potential cosmological probe.

In this context, Type Ia SNe play a special role. Thanks to the homogeneity of their luminosity, these thermonuclear explosions could be used as sharp distance estimators to measure the accelerated expansion of the universe (Riess et al., 1998; Perlmutter et al., 1999), leading to the discovery of dark energy. State-of-the-art SN Ia cosmological surveys have demonstrated that the intrinsic luminosity of SNe Ia only varies by about 0.1 mag (Betoule et al., 2014; Scolnic et al., 2018). Birrer et al. (2021) have shown the great benefit of these sharp distance indicators to break the mass-sheet degeneracy to improve the accuracy of the measurements of the Hubble constant from time delays.

Despite the great opportunity presented by having a lensed standard candle, the exploitation of lensed SNe poses an additional challenge: microlensing by stars (Dobler and Keeton, 2006). The intrinsic size of a SN is comparable to the Einstein radius of an individual star in the lens galaxy, a case analogous to microlensing of lensed quasars (Vernardos et al. 2023, in prep.). This means that observed magnification is sensitive to the – essentially unobservable – positions of stars in the lensing galaxy. Worse, as the supernova expands, the SN atmosphere crosses microlensing caustics. This causes a change in total magnification of the supernova and differential magnification across the atmosphere (Bagherpour et al., 2006; Goldstein et al., 2018; Huber et al., 2019; Mörtsell et al., 2020); this means that the light curves of each image can look quite different even though they are formed from the same background source, as illustrated in Fig. 4. This makes it a challenge for measuring accurate time delays between images, though early colour curves can overcome this due to an achromatic phase in the microlensing at early times (Goldstein et al., 2018; Huber et al., 2021b) as can spectroscopic observations of absorption lines in the SN atmosphere (Johansson et al., 2021; Bayer et al., 2021).

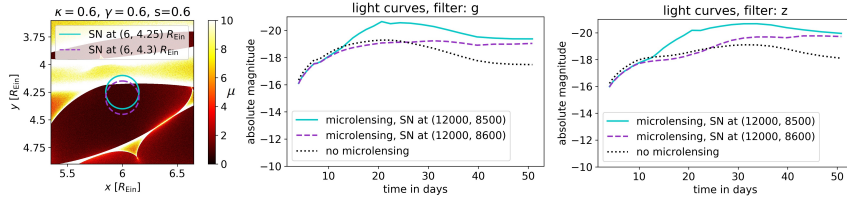


Fig. 4 Examples of Type Ia SNe light curves with significant microlensing. Left panel: a map of microlensing magnifications (μ , indicated by the color bar) on the source plane as a result from stars in the foreground lens galaxy. The map is for a lensed SN image with convergence $\kappa = 0.6$, shear $\gamma = 0.6$, and smooth dark matter fraction $s = 0.6$. In this example, the Einstein radius for the mean microlens is $R_{\text{Ein}} = 7.2 \times 10^{-3}$ pc. The two circles in solid cyan and dashed magenta indicate the size of a SN Ia at 21 rest-frame days after explosion. Middle and right panels: microlensed light curves in the g-band (middle panel) and z-band (right panel) corresponding to the SN positions shown in the left panel (solid cyan and dashed magenta). The intrinsic light curve without microlensing is shown in dotted black. When the expanding photosphere of the SN crosses a microlensing caustic with high μ , its light curve changes substantially relative to the no-microlensing case. Figure taken from Huber et al. (2019).

The SNe never reach a large enough size for the microlensing effect of multiple stars to average out, so microlensing makes it hard to standardise lensed SNe. The scale of this problem depends in detail on the magnification of the image, the type of the image (time-delay minimum, maximum or saddle) and fraction of density in stars at the location of the image. For high macro-magnification images, the scatter can be as large as 1 magnitude in flux (Schechter and Wambsganss, 2002; Yahalomi et al., 2017; Diego et al., 2022), entirely washing out the possibility of using lensed SNe as a standard candle. For images forming further from the Einstein Radius, and particularly for large mass systems where the dark matter fraction is higher at the Einstein radius, the scatter is much smaller and can be less than the intrinsic scatter of a Type Ia SN.

Foxley-Marrable et al. (2018) found that 20 percent of lensed SNe will contain an image with scatter comparable to the intrinsic scatter of a type Ia supernova luminosity, assuming the dark matter fractions of elliptical galaxies derived in Auger et al. (2010) and a Salpeter IMF. However, these standardisable images only form far beyond the Einstein radius of the lens. This means that the counter images are very close to the centre of the lens and demagnified. Measuring time delays will therefore be challenging, although the faint images arrive second so follow-up with a larger telescope may ameliorate this problem.

The 20 percent standardisable fraction is subject to two key caveats: the stellar initial mass function is assumed to be Salpeter-like and the ellipticity of the lensing mass follows that of the light. The assumption of a particular IMF sets the stellar-to-dark matter fraction. Fig. 5 shows the importance of this assumption: at very high stellar fraction there are no strongly lensed images with minimal microlensing scatter (Weisenbach et al., 2021). With a population of lensed SNe, Foxley-Marrable et al. (2018) find that observing the amount of microlensing induced scatter can be used to constrain the IMF of the lens galaxy, with strong sensitivity for lenses with Einstein radius between $0.2''$ and $0.5''$. The assumption that mass follows light produces more elliptical lens mass distributions than is seen in cold-dark-matter-only simulations. Increasing the ellipticity of the lens moves the dashed lines in Fig. 5 to the left. Strongly lensed images can form at

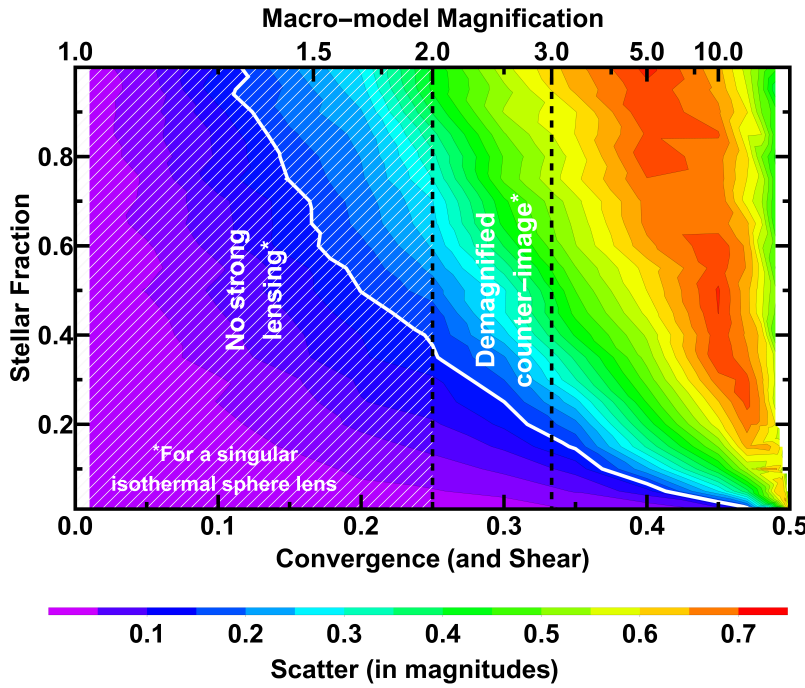


Fig. 5 Microlensing induced scatter (indicated by the color bar) for a point source lensed by a Singular Isothermal Sphere macromodel as a function of stellar fraction and macro-magnification. Scatter is lower for the lensed SN image that is far from the Einstein radius (with lower convergence/shear), but there is a limit since a convergence below 0.25 produces only single images (i.e., no strong lensing) and convergence below ~ 0.35 produces a faint counterimage (close to lens center) that makes time-delay measurements more challenging. Image credit: Luke Weisenbach, modified based on Weisenbach et al. (2021).

lower magnification, where microlensing is less significant. If real lenses are more spherical, then the standardisable fraction will fall. Therefore, the standardisation of lensed supernovae is subject to somewhat uncertain astrophysics. Exactly what we observe from a large sample of lensed supernovae will inform not just cosmology but also the astrophysics of matter in the strong lensing galaxy.

Despite microlensing distortions on the light curves of SNe and reductions in the number of standardisable SN, lensed SNe still have various advantages over the more conventional lensed quasars for time-delay cosmography. The drastically varying brightness of lensed SNe enable shorter monitoring campaigns (months) to obtain the light curves and thus more efficient measurements of time delays. Simulations of microlensed SN light curves with realistic photometric uncertainties showed that time delays can still be recovered accurately and precisely (Huber et al., 2019; Pierel and Rodney, 2019), and the dominant source of uncertainty in the time delays is typically photometric uncertainties rather than microlensing distortions (Huber et al., 2021a). Another advantage of lensed SNe is that SNe fade

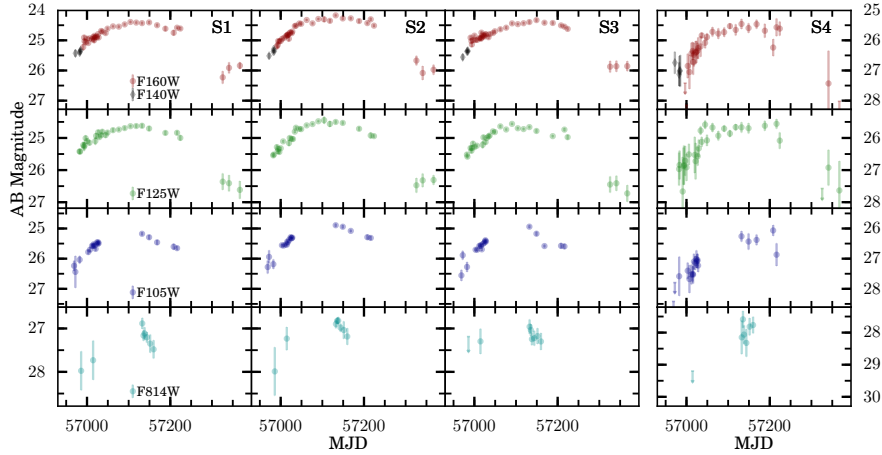


Fig. 6 Light curves of SN Refsdal from Hubble Space Telescope imaging in multiple wavelength filters. Each row consists of the light curves obtained in the specific filter that is indicated in the leftmost panel. Each column shows one of the four SN images, S1-S4 (left to right), that are indicated on the top panels. Each panel shows the observed AB magnitude as a function of the observer-frame days. Figure taken from Rodney et al. (2016).

after several months, revealing both the lens galaxy and the lensed SN host galaxy more clearly that enable more accurate lens mass modelling (e.g., Ding et al., 2021). In particular, spatially-resolved stellar kinematics of the foreground lens galaxy can be more readily acquired after the SN images fade, and the combination of lensing and kinematic data allows one to break the mass-sheet degeneracy (e.g., Barnabè et al., 2012; Yıldırım et al., 2020, 2021; Birrer et al., 2020; Shajib et al., 2023). Stellar kinematic maps of the lensed SN host galaxy would further constrain the lens mass distribution (Chirivì et al., 2020). We therefore anticipate lensed SNe to be an efficient cosmological probe in the upcoming era of time-domain astronomy when hundreds of such lensed SN events are expected to happen (e.g., Oguri and Marshall, 2010; Quimby et al., 2014; Goldstein et al., 2019; Wojtak et al., 2019).

2.2 Time-delay measurements

The time delays between multiple lensed images are a key ingredient for time-delay cosmography. The fractional uncertainties in the time delays translate directly to the fractional uncertainties in the $D_{\Delta t}$ and D_d measurements (Equation 1).

Traditionally, the measurements of time delays involve monitoring the lens system to acquire the light curves of either lensed quasars (e.g., Fassnacht et al., 2002; Courbin et al., 2018; Millon et al., 2020a,b) or lensed supernovae (e.g., Rodney et al., 2016; Dhawan et al., 2020). Fig. 6 shows an example of the light curves of the four images (S1, S2, S3 and S4) of SN Refsdal obtained by Rodney et al. (2016). Curve-shifting techniques that account for microlensing distortions are then applied to these light curves to extract the time delays (e.g., Tewes et al., 2013; Pierel and Rodney, 2019; Millon et al., 2020c). By making use of the characteristic SN Ia SEDs, Dhawan et al. (2020) used SN Ia template light curves to fit to the HST

images of iPTF16geu and measured the 3 independent time delays between the four SN images. New machine learning approaches such as random forests are also being developed to infer the delays of microlensed SN Ia systems from the light curves (e.g., Huber et al., 2021a).

SNe are not only drastically changing their brightness, but their spectra also evolve substantially. The spectroscopic evolution of supernovae offers a new avenue to measure the time delays that are complementary and competitive to the light-curve techniques, as demonstrated by Johansson et al. (2021) for the case of iPTF16geu. The photospheric velocity in SNe Ia evolves with time as $v(t) \propto t^{-0.22}$ (Piro and Nakar, 2014), which allows the use of spectral dating to constrain the time delay between images, especially at early times when the velocities of the spectral features is high and the changes from day-to-day are significant. For the most common type of core-collapse supernovae, SNe IIP, where the light curves rise fast to peak and then reach a plateau phase that could last for hundreds of days, spectral time delays may be the best way forward. Fig. 7 shows an example of the spectra of Type IIP SN1999em from the TARDIS simulation (Kerzendorf and Sim, 2014; Vogl et al., 2019, 2020) at multiple epochs after explosion (Bayer et al., 2021). These epochs (in rest-frame days) are in the plateau phase of this Type IIP SN. The spectra show prominent absorption lines, especially H β , FeII and H α that are indicated on the figure, and the absorption wavelength increases as a function of time. It is precisely such evolutions in the spectral features that allow us to infer the time delays between two SN images.

In more detail, a sequence of spectra of the first appearing SN image, say SN image A (such as those shown in Fig. 7) yields the absorption wavelength of each spectral feature as a function of the SN phase (days after explosion). When we obtain a single spectra of a trailing SN image, say SN image B, and measure the absorption wavelength of the same spectral feature, we can determine the phase of SN B by using the relation between the absorption wavelength and phase from SN A. The determined phase of SN B relative to SN A, together with the known observational times of the epochs, then allows us to compute the time delays between SN images A and B. Microlensing of SN introduces scatter in the relation between the absorption wavelength and phase, and this effect can be quantified using microlensing maps such as those from the GERLUMPH software (Vernardos and Fluke, 2014; Vernardos et al., 2014, 2015). Accounting for the effect of microlensing that distorts spectra, Bayer et al. (2021) have shown that this technique can yield time delays with uncertainties of ~ 2 days per spectral feature with signal-to-noise in the spectra of ~ 20 per wavelength bin of 3\AA width. With multiple spectral features and epochs, the inferred time delays from such spectral approach will be even more precise and accurate.

2.3 Cosmography with lensed SNe: present cosmological constraints and future forecasts

Of the five known lensed SN systems with spatially resolved SN images, SN Refsdal is the most promising system in delivering a precise and accurate H_0 measurement (with $<10\%$ uncertainty) in the near future. As mentioned in Section 1, the measurement of the time delay of image SX relative to the first image S1 is forthcoming, and is expected to have uncertainties of only a few percent (P. Kelly,

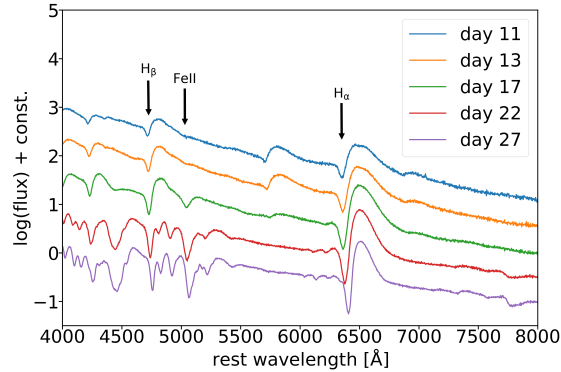


Fig. 7 Spectral evolution of core-collapse SN1999em based on the TARDIS simulation from Vogl et al. (2019, 2020). Three prominent spectral features, $H\beta$, FeII and $H\alpha$, are labelled. The SN phases are indicated by their rest-frame days after explosion. As the SN phase increases, the spectral features become stronger and the absorption wavelengths increase. Such a sequence of spectra of the first-appearing SN image provides the wavelength-phase relation, and a measurement of the absorption wavelength of a trailing SN image therefore provides information of its SN phase and thus its time delay relative to the first-appearing SN image. With each spectrum of signal-to-noise of 20, Bayer et al. (2021) showed that the time delays can be measured with uncertainties of ~ 2 days per spectral feature, even after accounting for the effects of microlensing. Figure taken from Bayer et al. (2021).

private communications). For a preview of the constraining power on H_0 from SN Refsdal, Fig. 8 shows a forecast of the inferred H_0 for a range of hypothetical time-delay measurements of image SX relative to image S1, assuming the flat Λ CDM cosmological model (Grillo et al., 2020). These are based on cluster mass models of Grillo et al. (2020) that incorporate all known sources of uncertainties. We anticipate that a 3% uncertainty on SX time delay would yield approximately 6% and 40% uncertainties (1σ , including both statistical and systematic) for H_0 and Ω_m , respectively.

Various studies indicate that current and future surveys would discover dozens to hundreds of lensed SNe (Goobar et al., 2002; Oguri and Marshall, 2010; Goldstein et al., 2019; Wojtak et al., 2019; Pierel et al., 2021). In particular, Oguri and Marshall (2010) anticipated thousands of lensed quasars and ~ 100 lensed SNe to be detected in the Rubin Observatory Legacy Survey of Space and Time (LSST; LSST Science Collaboration et al., 2009). Using a mock sample of ~ 1500 well-observed lenses (consisting of 1476 lensed quasars and 66 lensed SNe) and assuming Planck priors in a flat Universe, Oguri and Marshall (2010) expected the following 1σ uncertainties on cosmological parameters: $\sigma(w_0) = 0.15$, $\sigma(w_a) = 0.41$ and $\sigma(h) = 0.017$ where (w_0, w_a) are the time-independent and time-dependent components of the dark energy equation-of-state parameter, and h is H_0 in units of $100 \text{ km s}^{-1} \text{ Mpc}^{-1}$.

Huber et al. (2019) analyzed in detail the number of lensed SNe Ia that could yield time-delay measurements with precisions better than 5% and accuracies better than 1%, with realistic microlensed SN Ia light curves and LSST observing strategies. While LSST is efficient at detecting lensed SNe given its wide survey area and depth, the observing cadence per filter is not rapid enough to map out light curves for precise delay measurements. Follow-up observations at the cadence

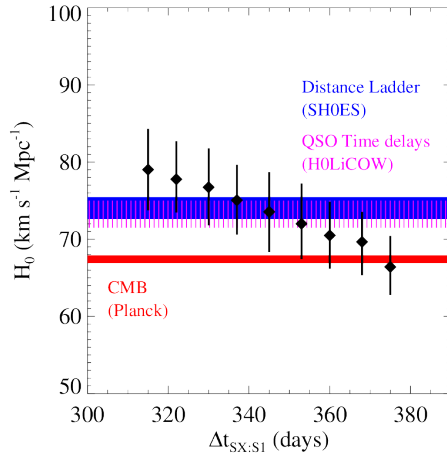


Fig. 8 Forecast of H_0 from SN Refsdal as a function of the time delay between SN images SX and S1, using the reference mass model of Grillo et al. (2020). The median values of H_0 (diamonds) with the 1σ uncertainties in flat Λ CDM are shown for 9 different hypothetical SX-S1 delays, each with an assumed uncertainty of 10 days. For comparison, the blue, magenta and red bands show, respectively, the 1σ credible intervals from SH0ES (Riess et al. 2019), H0LiCOW (Wong et al. 2020) and Planck (Planck Collaboration et al. 2020). Figure taken from Grillo et al. (2020).

of at least one epoch every 2 days would drastically increase the number of lensed SNe with “good” time delays (i.e., those delays with uncertainties $<5\%$ in terms of precision and $<1\%$ in terms of accuracy). Based on the results of Huber et al. (2019), Suyu et al. (2020) simulated a sample of 20 lensed SNe Ia from LSST that are expected to have good time delays. Assuming that these systems would have high-resolution imaging and spatially resolved kinematic measurements to break the mass-sheet degeneracy and yield 6.6% uncertainty on $D_{\Delta t}$ and 5% uncertainty on D_d , this modest sample of 20 lensed SNe Ia could yield constraints on H_0 and Ω_m of 1.3% and 19%, respectively, in flat Λ CDM, as illustrated in Fig. 9. In an open Λ CDM cosmology (i.e., allowing for a spatially curved Universe), a similar constraint on H_0 compared to flat Λ CDM is achievable, while in the flat w CDM cosmology (where the dark energy equation-of-state parameter w is allowed to vary), the H_0 constraint degrades to 3% (Suyu et al., 2020).

The forecast made by Suyu et al. (2020) did not make use of the standardisable nature of SNe Ia, due to the effects of microlensing and millilensing as mentioned in Section 2.1. Nonetheless, Foxley-Marrable et al. (2018) showed that lensed SNe Ia with asymmetric configurations, i.e., with a SN image located far outside the Einstein radius of the foreground lens, have low microlensing scatter of $\lesssim 0.15$ mag for the outer SN image, which is comparable to the intrinsic dispersion of a typical SN Ia. These systems are thus standardisable in terms of overcoming microlensing perturbations, and Foxley-Marrable et al. (2018) estimated that about $\sim 22\%$ of the ~ 930 LSST systems predicted by Goldstein et al. (2018) would be standardisable. However, Goldstein et al. (2018) estimated that only ~ 650 systems would be detected early enough by LSST to deliver reliable time delays. This implies a sam-

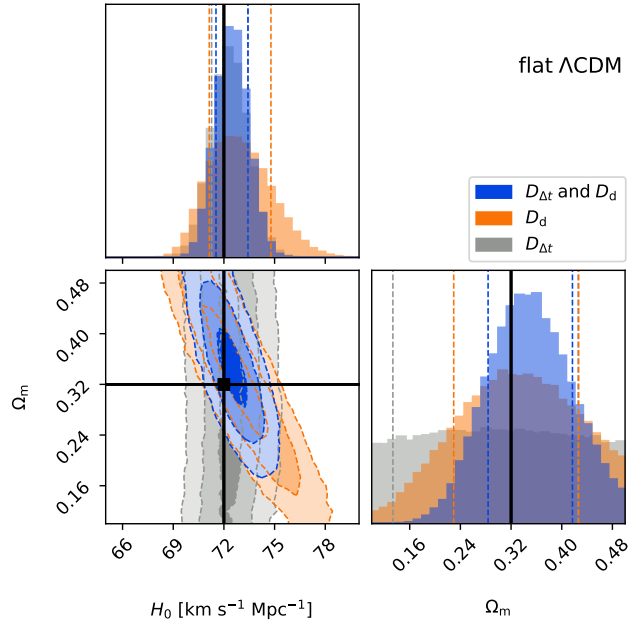


Fig. 9 Forecast of constraints on H_0 and Ω_m in flat Λ CDM from a sample of 20 lensed SNe Ia from LSST with precise and accurate time-delay measurements. Assuming distance measurements of $D_{\Delta t}$ and D_d with 6.6% and 5% uncertainties, respectively, for each lensed SN Ia, this modest sample is expected to yield H_0 and Ω_m with precisions of 1.3% and 19%, respectively. Figure taken from Suyu et al. (2020).

ple of ~ 140 lensed SNe Ia that are standardisable and with potential time-delay measurement.

Following the estimates of Foxley-Marrable et al. (2018) and by making use of 144 standardisable lensed SNe Ia, Birrer et al. (2021) combined non-lensed SNe Ia with lensed SNe Ia via a Bayesian hierarchical framework to infer the constraints on H_0 . The aim is to use the standardisable nature of SNe Ia to break the mass-sheet degeneracy, without using spatially resolved kinematics of the lens galaxy. Assuming optimistically that the time delays between SN image pairs can be measured with a precision of 2 days for all these systems and that the typical Einstein radius is $\sim 1''$, Birrer et al. (2021) found that H_0 can be measured with an uncertainty of 1.5%.

The various cosmological forecasts depend sensitively on assumptions of follow-up observations in order to classify the SN type, measure the time delays, acquire high-resolution imaging and spectroscopy. As described in Section 2.1, these are necessary for measuring absolute distances to lensed SNe and using them as a cosmological probe. In Section 4.4, we discuss in more detail the follow-up requirements for lensed SNe.

3 Astrophysical probe

Lensed SNe are powerful astrophysical tools to study supernovae and galaxies, in addition to probing cosmology through their time delays.

In Section 3.1, we explain how lensed SNe provide an excellent opportunity to constrain SN progenitors. In Section 3.2, we describe how lensing magnifications enable the acquisition of high-redshift SN spectra that are crucial for SN cosmology. In Section 3.3, we outline the use of microlensing to probe SN structure. In Section 3.4, we show lensed SNe as a probe of dust in the foreground lens galaxy.

3.1 SN physics and progenitors

Whilst it is accepted that a Type Ia SN is a thermonuclear detonation of a white dwarf (WD), the cause of the detonations remains uncertain even after decades of study (Maoz et al., 2014; Livio and Mazzali, 2018).

The classic progenitor model (often referred to as the single degenerate channel) for a Type Ia SN is a close binary of a white dwarf and a post main sequence star (Whelan and Iben, 1973). As the star expands, it overflows its Roche lobe and its outer layers are accreted onto the WD until the WD reaches the Chandrasekhar mass. At this point, electron degeneracy pressure can no longer support the WD, and gravitational collapse causes thermonuclear detonation of the WD. This model is attractive, since it naturally explains the standardisability of SNe Ia, with the progenitor always having the same mass and near identical composition. However the lack of evidence for surviving companions suggest that this channel cannot account for all SNe Ia (González Hernández et al., 2012; Lundqvist et al., 2015).

An alternative progenitor model is the double degenerate channel. Here two white dwarfs merge, exceeding the Chandrasekhar mass (Iben and Tutukov, 1984; Webbink, 1984). This mechanism leaves behind no companion star, but since each pair of white dwarfs will sum to a different mass, there is no obvious reason why this channel would produce a good standard candle. In addition to these two classic channels of single- and double-degenerate systems, there are other explosion mechanisms that have been explored, including sub-Chandrasekhar explosions (e.g., Sim et al., 2010), delayed detonations (e.g., Röpke et al., 2012), and double detonations of sub-Chandrasekhar WDs (e.g., Fink et al., 2007).

Early observations of SN light curves are critical in constraining the properties of SN progenitor systems (e.g. Kasen 2010; Piro et al. 2010; Rabinak and Waxman 2011; Nugent et al. 2011; Bloom et al. 2012; Goobar et al. 2015; Piro and Morozova 2016; Noebauer et al. 2017; Kochanek 2019; Fausnaugh et al. 2019; Yao et al. 2019; Miller et al. 2020; Bulla et al. 2020). If non-degenerate matter is close to the WD, then it should be shock heated by the explosion, producing excess high energy flux in the first few hours to days of the light curve. In addition to SNe Ia, early observations of core-collapse SNe are also helpful in constraining the properties, such as the sizes, of the progenitor stars (e.g., González-Gaitán et al., 2015; Chen et al., 2022). Even with the development of wide-field optical surveys, observing these earliest moments of SNe is heavily reliant on chance. Strong lensing gives us the opportunity to predict the precise reappearance time of a SN, such that very early data can be gathered (Suwa, 2018; Suyu et al., 2020).

There are multiple challenges to this approach: early detection of the first SN image, possible image demagnification, distortions of SN light curves and spectra by microlensing, and time delay predictions of insufficient precision. We discuss each of these in turn.

Detection of a lensed SN based on only the appearance of the first image is more difficult, due to possible confusions between a lensed and an unlensed SN without the multiple SN images present. This confusion can be overcome when the lensed SN host galaxy is visible as lensed arc features in addition to the foreground lens galaxy.

Whilst lensed SNe will be discovered from highly magnified images, images occurring with significant time delay after the bright “discovery image” are typically demagnified in the case of two-image systems (Foxley-Marrable et al., 2020). The situation is better for four-image systems where some of the trailing SN images can be brighter than the discovery SN image. We expect $\sim 2/3$ of the lensed SNe to be two-image systems, and $\sim 1/3$ to be four-image systems (Oguri and Marshall, 2010).

As seen in Fig. 4 and shown in Huber et al. (2019), microlensing distorts the SN light curves and spectra, potentially garbling the information on progenitors. Encouragingly, Suyu et al. (2020) have investigated the microlensing effects on four different explosion models of SNe Ia and demonstrated that spectral distortions due to microlensing are $\lesssim 1\%$ at the 1σ level within 10 rest-frame days after explosions. Therefore, microlensing is expected to have negligible impact on early-phase spectra (within ~ 10 rest-frame days) for deciphering SN progenitors.

Finally, time delays cannot be precisely estimated from lens modelling alone. A 5–10 percent precision is typical from the best lens models (e.g., Shajib et al., 2019), and the uncertain value of the Hubble constant given the discrepant H_0 measurements (e.g., Verde et al., 2019; Di Valentino et al., 2021) adds several more percent of uncertainty in the predicted time delays. For systems with delays $\gtrsim 20$ days that are sufficiently long to catch the trailing SN images from their beginnings (given the time it takes to detect the first SN image and to arrange follow-up observations), a 10% uncertainty would translate to $\gtrsim 2$ days. Given this uncertainty, the predicted delay can easily miss the observations within ~ 2 days after explosion, the crucially early moments for constraining SN progenitors.

To overcome these challenges, deep and high-cadence (ideally daily) monitorings with imagers after the detection of the first appearing SN image would greatly help. Such a monitoring would acquire the early-phase light curves of trailing SN images, and spectroscopic observations of the early phases can be triggered as soon as a trailing SN image appears in the monitoring. Early-phase spectroscopic observations especially in the rest-frame UV are unprecedented and important for constraining SN progenitors (Suyu et al., 2020). The time delays of lensed SNe provide a unique and exciting avenue to acquire such spectroscopic observations for studying SN progenitors.

3.2 High-z SN spectra through gravitational telescopes

The precision of SNe Ia as distance indicators, and thus their use to accurately constrain the nature of dark energy, is ultimately limited by our understanding of progenitor systems, e.g., the potential evolution of the SN properties, especially

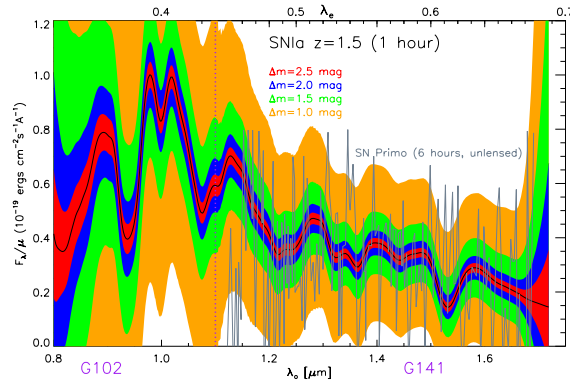


Fig. 10 Expected signal for HST observations through grisms G102 and G141 of a SN Ia at $z = 1.5$ for different magnifications provided by lensing. The shaded regions in [orange, green, blue, red] indicate the 1σ uncertainty per pixel in one-hour-long exposures for $\Delta m = [1, 1.5, 2.0, 2.5]$ mag of magnification, respectively. The observed spectrum of “SN Primo” (Rodney et al., 2012, six hours exposure time) is also shown for comparison.

their absolute magnitude, over cosmic time. Thus, confirming the standard-candle nature through spectroscopic comparisons between SNe near and far is essential. With current instruments, detailed comparisons beyond $z > 1$ are not possible, due to the low SNR. This will remain challenging in the James Webb Space Telescope (JWST) era. However, multiple spectra of SNe at high redshift are required to check if the progenitor population evolves with redshift. Hence, the magnification of the signal from gravitational lensing could become essential to constrain one of the biggest systematic uncertainties in SN Ia cosmology (Petrushevska et al., 2017; Johansson et al., 2021). Fig. 10 shows the noisy HST spectrum, based on six hours of observations of SN “Primo” at $z = 1.55$ observed by Rodney et al. (2012) compared with the expected signal if observed for shorter time through gravitational telescopes of different strengths, $\Delta m = 1, 1.5, 2.0$ and 2.5 mag, where Δm is the difference in magnitude coming from lensing magnification. These magnifications are expected to be typical for lensed SNe (Goldstein et al., 2019).

3.3 SN structure with microlensing

When a background source crosses a caustic network produced by microlenses, this allows one to estimate the physical dimensions of the light emitting surface, most robustly its half-light radius (Mortonson et al., 2005; Vernardos and Tsagkatakis, 2019). For the case of SNe, their expanding ejecta lead to an increasing size that is directly linked to the expansion velocity. Because the (unobservable) distance from a caustic/high magnification region on the source plane is inversely proportional to changes in brightness due to microlensing, deformed SN light curves, like the ones shown in Fig. 4, can be used to constrain the size evolution, and subsequently the expansion velocity. In combination with the measurements of the photospheric velocity of the SN ejecta from spectroscopic observations, the SN size evolution can provide information on SN explosion models. We illustrate the size measurement via microlensing by the following toy model.

Let us assume that the brightness of a lensed SN image at any given time t and wavelength λ (ignoring time delays and macromagnification for simplicity) is:

$$I(t, \lambda) = \int dx \int dy S(x, y; t, \lambda) \mu(x, y), \quad (6)$$

where S is the two dimensional intrinsic SN brightness profile, μ is the microlensing magnification on the source plane, and the integrals are performed over the extent of the source brightness profile. Assuming, for illustrative purposes, that the intrinsic surface brightness profile (S) is a circle of radius $R(t)$ with a known, constant surface brightness $i(t, \lambda)$, we get:

$$I(t, \lambda) = i(t, \lambda) \int_0^{2\pi} \int_0^R \mu(r, \theta) r dr d\theta = i(t, \lambda) F(R) \quad (7)$$

in polar coordinates (r, θ) , where the value of the integral can be written as a radius and time-dependent factor, $F(R)$, and whose probability distribution can be calculated numerically from magnification maps. In fact, we can drop the assumption on a uniform profile and perform the convolution in Equation (6) for different profile shapes. Therefore, if we know $S(x, y; t, \lambda)$ from a standardised SN type and calculate F , then we can measure $R(t)$. If the SN brightness profile shape varies over time, ratios of $I(t, \lambda)$ can be considered for separations in time Δt small enough so that the profile does not change by much. Finally, we note that Dobler and Keeton (2006) have used a similar approach, the time-weighted light curve derivative, albeit to measure the stellar mass fraction of the lensing galaxy.

In an analogous way, the relative size, or more specifically the half-light radius, of the SN ejecta at different wavelengths can be estimated from Equation (6). Actually, the shape of the SN profile and/or the expansion velocity may vary in different wavelengths (see Figs. 11 and 12; Huber et al., 2019; Bayer et al., 2021), leading to different half-light radii (i.e., $R = R(t, \lambda)$ instead of $R(t)$). In the context of our toy model, the brightness ratio between two wavelengths at a given time t can be used to constrain the relative half-light radii:

$$\frac{I(t, \lambda_1)}{I(t, \lambda_2)} = \frac{i(t, \lambda_1)}{i(t, \lambda_2)} \frac{F(R_1)}{F(R_2)}. \quad (8)$$

Such measurements of radii across wavelengths and time not only provide a check on whether the expansion is homologous (when comparing the radii to the measured velocities from spectra), but also information on the explosion models that alter the dependence of radius on wavelength. It remains to be seen whether microlensing constraints on explosion models are competitive to the existing constraints based on SN spectral evolution modelling and analysis.

3.4 Dust properties in distant galaxies

The different sightlines of multiple images offer unique opportunities to explore the properties of the interstellar medium of the deflecting galaxy, as was first shown for strongly lensed QSOs by Falco et al. (1999) and in subsequent studies (e.g., Elíasdóttir et al., 2006; Østman et al., 2008; Hjorth et al., 2013). This is important as accurate measurements of e.g., the total-to-selective extinction parameter $R_V \equiv$

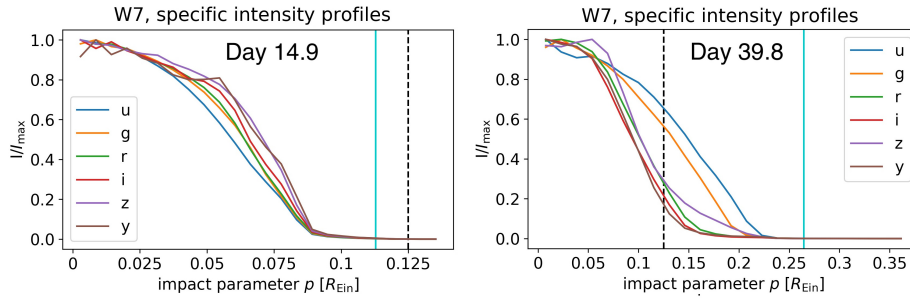


Fig. 11 Specific intensity profile of the W7 explosion model of SNe Ia. Left: radial intensity profiles in different filters 14.9 rest-frame days after explosion, in units of the Einstein radius of the microlenses ($R_{\text{Ein}} = 2.2 \times 10^{16}$ cm for this specific case). The vertical solid cyan lines indicate the radius that encloses 99.9% of the total projected specific intensity. The vertical black dashed lines are random locations of caustics – effects of microlensing are strong when the specific intensity of the SN crosses a caustic. Right panel: same as the left panel but for a SN Ia 39.8 rest-frame days after explosion. Figure extracted and modified from Huber et al. (2019).

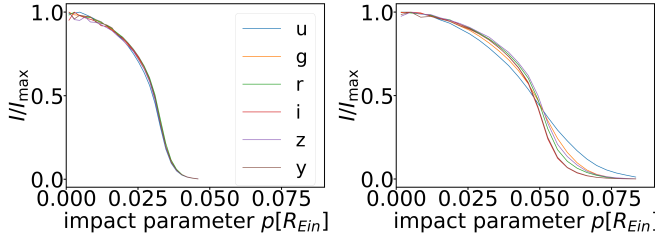


Fig. 12 Specific intensity profiles from TARDIS (Kerzendorf and Sim, 2014; Vogl et al., 2019) modelling of SN 1999em, a Type IIP SN (Vogl et al., 2020) projected on the plane of the sky (Bayer et al., 2021). Left: radial intensity profiles in different filters 11 rest-frame days after explosion, in units of the Einstein radius of the microlenses ($R_{\text{Ein}} = 2.9 \times 10^{16}$ cm for this specific case). Right panel: same as the left panel but for 27 rest-frame days after explosion. Figure taken from Bayer et al. (2021).

$A_V/E(B - V)$, a key number for many areas of astronomy, are very hard to establish outside the Milky Way and the Magellanic Clouds. The *extinction* in the V-band, A_V , is defined as

$$A_V := m_V - m_{V,0}, \quad (9)$$

where m_V is the apparent magnitude with dust extinction and $m_{V,0}$ is the intrinsic magnitude without dust extinction. The extinction for any other wavelength band is defined in a similar way. The *color excess* (or reddening) between the B and V band is

$$E(B - V) := A_B - A_V \quad (10)$$

$$= (m_B - m_V) - (m_{B,0} - m_{V,0}). \quad (11)$$

In the case of no dust extinction, then $A_V = 0$, $A_B = 0$ and $E(B - V) = 0$. For a fixed R_V value, higher A_V values (or higher $E(B - V)$ values) correspond to more dust along the sight line. The observed colors in multiple bands of the images

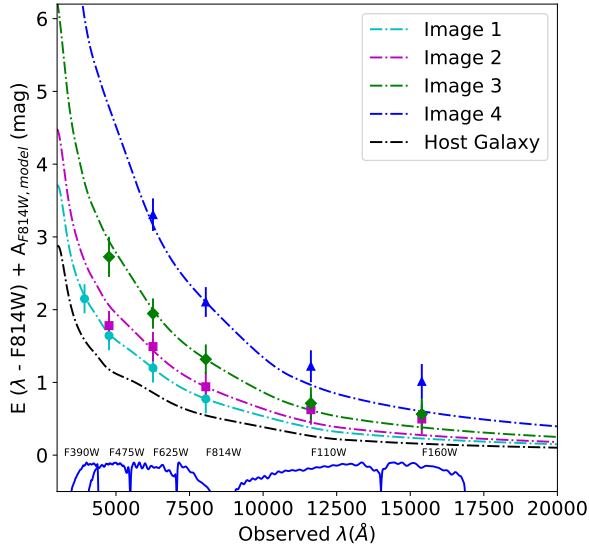


Fig. 13 The observed color excess for the resolved images from HST of iPTF16geu as a function of wavelength. The absorption from the host galaxy dust grains is plotted in black. For Image 1 we can see that the host galaxy is the dominant source of extinction, and for images 2, 3, 4 there is a progressively larger contribution from the dust in the lens galaxy, with correspondingly higher values of the color excess. Figure taken from Dhawan et al. (2020).

are used to infer the differential reddening as the various images travel through different regions of the lensing galaxy (i.e., infer the differences in A_V between the multiple SN images). Corrections for differential extinctions in systems of strongly lensed SNe Ia is crucial to also make use of their standard candle nature to infer the lensing magnification.

Exploiting the well-known color evolution of SNe Ia, Dhawan et al. (2020) were able to infer both the extinction in the lensing galaxy for iPTF16geu, along with the common color excess from attenuation in the host galaxy using multi-band images from HST, as shown in Fig. 13. For iPTF16geu, with an impact parameter of about 1 kpc, two of the images (3 and 4) suffered significant extinction and the total magnification inferred from spatially unresolved images was significantly underestimated. Intriguingly, the best fit values of R_V for the lensing galaxy at $z = 0.216$ were much lower than what is observed for studies of stars in the Milky-Way (Schlafly et al., 2017), but similar to what is found in studies of well-measured, highly-reddened SNe Ia (Amanullah et al., 2015).

4 Searches and Rates

4.1 Methods

There are multiple ways to find lensed supernovae by making use of their image morphology, magnification, image multiplicity and/or time evolution. We briefly describe several approaches in this subsection.

4.1.1 Search through known lensed galaxies

A straightforward approach to find lensed SNe is to monitor known lensed galaxies and wait for a SN to explode in one of the lensed galaxies (Shu et al., 2018). Using the sample of 128 galaxy-scale strong-lens systems from the Sloan Lens ACS Survey (SLACS; Bolton et al., 2006, 2008), the SLACS for the Masses Survey (S4TM; Shu et al., 2017), and the Baryon Oscillation Spectroscopic Survey Emission-Line Lens Survey (BELLS; Brownstein et al., 2012; Bolton et al., 2012), Shu et al. (2018) estimated that the rates of strongly lensed SNe Ia and core-collapse SNe are 1.23 ± 0.12 and 10.4 ± 1.1 events per year, respectively.

One can either monitor known lens systems (especially ones with the highest star-formation and SN rates) through dedicated observing programs (Craig et al., 2021), or through wide-field imaging surveys such as the ongoing ZTF (Bellm et al., 2019). In the latter case, lens systems and lens candidates can be cross matched to transient alerts from ZTF through various brokers such as AMPEL (Nordin et al., 2019), ANTARES (Saha et al., 2014; Narayan et al., 2018; Lee et al., 2020; Matheson et al., 2021) and Lasair (Smith et al., 2019). Multi-epoch images of lens candidates can also be used to find lensed SNe based on temporal and spatial information of transients occurring near the lens candidates (Sheu et al., 2023). There are now thousands of confirmed and candidate lens systems from a wide range of lens searches, notably through machine learning approaches in recent years (e.g., Bolton et al., 2006; Limousin et al., 2009; Gavazzi et al., 2012; Brownstein et al., 2012; Vieira et al., 2013; Cañameras et al., 2015; Jacobs et al., 2017, 2019; Marshall et al., 2016; More et al., 2016; Sonnenfeld et al., 2018, 2020; Petrillo et al., 2019; Cañameras et al., 2020, 2021; Huang et al., 2020, 2021; Savary et al., 2022; Rojas et al., 2022; Shu et al., 2022; Tran et al., 2022). However, given the relatively shallow limiting depth of $r = 20.6$ mag (5σ) of the ZTF survey (Bellm et al., 2019), individual lensed SN images associated with the lensed galaxies are likely below the detection threshold (Oguri and Marshall, 2010; Wojtak et al., 2019). Nonetheless, the combination of the flux from all lensed SN images can be above the detection threshold, which motivates the next search approach through magnifications.

4.1.2 Search through lensing magnification

While targeted searches for lensed SNe in known strongly lensed systems is straightforward, it is also constraining given the limited number of such systems. Since supernovae, especially SNe Ia, have a known narrow range of intrinsic brightness, it is feasible to identify particularly bright SNe as potential lensing candidates.

Quimby et al. (2014) proposed a technique to find unresolved lensed images of SNe Ia based on their high magnification and colors. Lensed SNe are expected

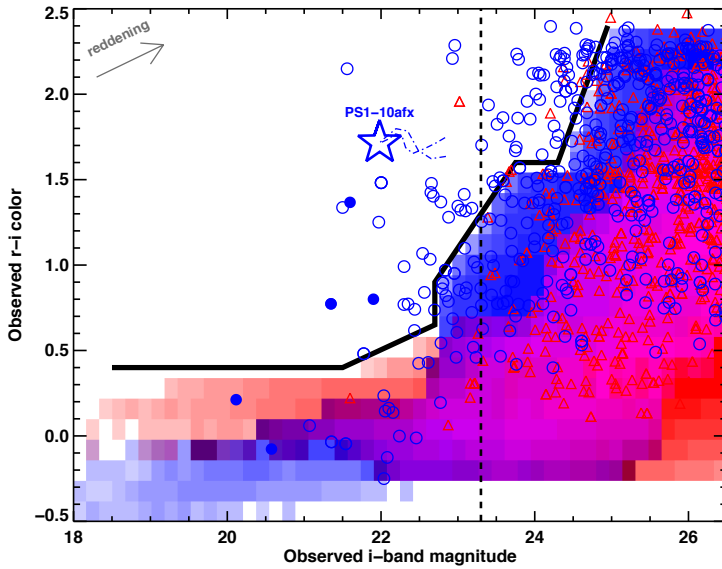


Fig. 14 The expected distribution of unlensed SNe population (SNe Ia in blue shaded, and core-collapse SNe in red shaded) is enclosed by thick black line showing the red limit. The lensed population predicted by Monte Carlo simulations is shown for SNe Ia (blue circles) and core-collapse SNe (red triangles). Vertical line marks the single epoch limit for LSST. Figure taken from Quimby et al. (2014).

to come from high redshifts where they will be in larger numbers owing to a larger volume and the lensing probability being higher for distant sources. The lensing magnification will make them appear brighter but their colors will largely be unaffected. Hence, in a color-magnitude diagram, the lensed SNe Ia will appear redder, at given magnitude, since they will be originating from higher redshifts compared to the unlensed population (see the blue circles above the black solid line in Fig. 14).

Another technique is based on having some knowledge of the redshifts of the galaxies involved, and it is interesting since it does not require multiple images to be spatially resolved. Thus it can in principle be used to detect arbitrarily compact systems, complementing other techniques, and allowing to probe the entire angular separation distribution of strongly lensed systems.

Fig. 15 from Goobar et al. (2017) shows a practical realisation of detecting unresolved strongly lensed supernova: iPTF16geu was found to be a 30σ outlier when compared with other SNe Ia at the same redshift. Thus, even with the very modest $\sim 2''$ spatial resolution at the 48-inch telescope at the Palomar Observatory, a strongly lensed system with $\theta_E = 0.3''$ could be identified. The difficulty with this approach is that spectroscopic observations are needed for classification of the transients, along with obtaining reliable redshifts of the galaxies, potentially a daunting task for large surveys with tens or even hundreds of new astrophysical transients found every night.

Goldstein and Nugent (2017) proposed a methodology to lower the rate of false positives: only considering transients spatially associated with elliptical galaxies,

which make up about $\sim 80\%$ of the galaxy lenses and typically only host SNe Ia, including the sub-luminous ones. Furthermore, thanks to prominent 4000Å breaks, robust photometric redshifts can be computed for elliptical galaxies. Hence, if the transient appears to be too bright for being a SN Ia at the (photometric) redshift of the nearest galaxy, there is a good chance that it is a deflecting galaxy, as opposed to the host. Upon a secure identification, targeted high spatial-resolution imaging can be used to try to resolve the system.

4.1.3 Search through multiplicity of images

For imaging surveys with faint limiting depth and good angular resolution such as the upcoming LSST, the multiple SN images of a lensed SN can be resolved and detected individually. Oguri and Marshall (2010) and Wojtak et al. (2019) investigated the number of lensed SNe detectable from such an approach. Specifically, Wojtak et al. (2019) imposed the following conditions for detecting a lensed SN via its image multiplicity: (1) the maximum image separation between the multiple SN images is between 0.5'' and 4'', where the lower limit is set by the expected seeing of LSST and the upper limit puts focus on galaxy-scale lens systems, (2) the flux ratio between the two images of a two-image (double) system is larger than 0.1, in order to have good contrast and clear identification of the images, and (3) at least three of the four images in a quad system are detected, and both images of a double system are detected.

For surveys with limiting magnitude that are fainter than ~ 23 mag in g, r or i-band, the detection via image multiplicity is expected to detect more lensed SN systems than the magnification approach. We illustrate this in Fig. 16 for lensed SNe Ia, and refer to Wojtak et al. (2019) for other types of lensed SNe that show similar trends. A combination of the two complementary approaches (magnification and multiplicity), as labelled by ‘‘hybrid’’ in Fig. 16, delivers more lens systems than the individual approaches on their own. In terms of cosmological applications, the multiplicity approach tends to detect lensed SN systems with longer time delays and larger image separations, which are more suitable for time-delay cosmography.

4.1.4 Search through spatio-temporal images

Most of the lensed SN searches in ZTF are based on the approaches of cross matches to lens systems/candidates (Section 4.1.1) or magnification (Section 4.1.2) since the angular resolution of ZTF (with 1'' pixel sizes) does not resolve the multiple SN images of typical lens systems. However, in the advent of LSST, there will be high angular-resolution and deep images with at least hundreds of epochs per filter at each sky location. Building upon the image multiplicity method described in Section 4.1.3, Kodi Ramanah et al. (2021) proposed a machine-learning approach to classify an object based on images from cadenced surveys like the Young Supernova Experiment (YSE; Jones et al., 2021) and LSST. Machine learning techniques such as convolutional neural networks (CNN) perform well and are efficient at processing large amounts of imaging data for finding gravitational lenses (e.g., Jacobs et al., 2017, 2019; Lanusse et al., 2018; Metcalf et al., 2019; Petrillo et al., 2019; Cañameras et al., 2020, 2021). The spatio-temporal method of Kodi

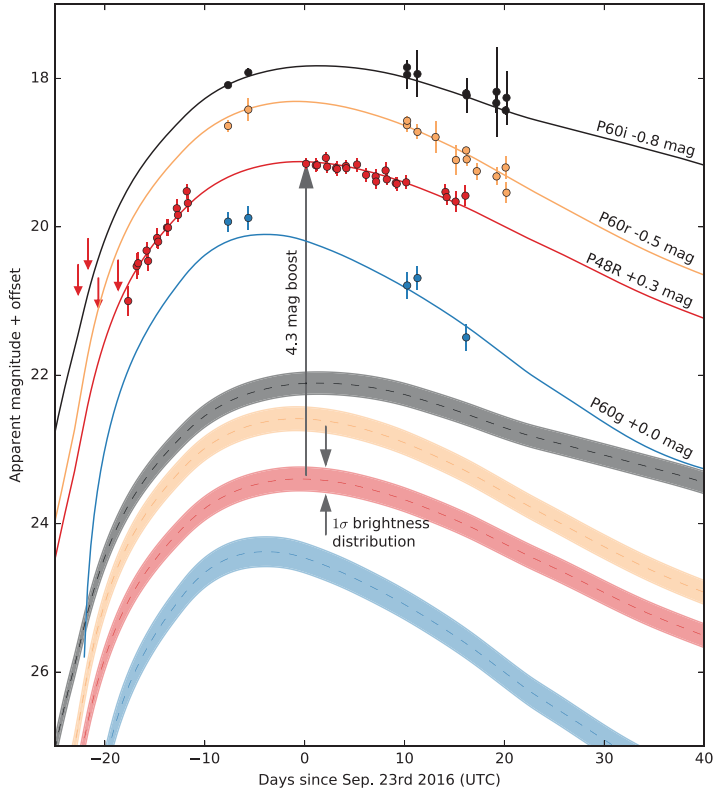


Fig. 15 Multicolor light curve of iPTF16geu showing that the unresolved supernova was 4.3 magnitudes (30 standard deviations) brighter than expected for its redshift. The magnitudes are measured with respect to time of maximum light in the R-band at P48 and in the g-, r-, and i-bands with the P60 telescope. The solid lines show the best-fitted SN Ia model to the data, while the dashed lines indicate the expected light curves at $z = 0.409$ (without lensing). The bands represent the standard deviation of the brightness distribution for SNe Ia. To fit the observed light curves, a brightness boost from gravitational lensing of 4.3 magnitudes is required. Figure from Goobar et al. (2017).

Ramanah et al. (2021) builds upon the success of the CNN and incorporate also time-domain information.

Rather than providing a neural network with the multi-band stacked (static) images of objects for classification, Kodi Ramanah et al. (2021) developed a network to take in a temporal series of images. The network architecture is a CNN that encodes long short-term memory (LSTM, a type of recurrent network; Sher-

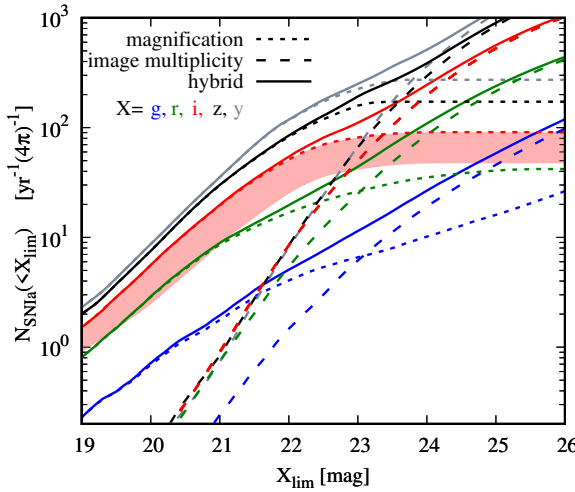


Fig. 16 The number of lensed SNe Ia expected per year over the whole sky as a function of the imaging survey limiting magnitude depth. The different colors correspond to detection in different filters (g , r , i , z or y). The dotted (dashed) lines show the expected number of lensed SNe Ia detected through the magnification (image multiplicity) approach. The hybrid approach, a combination of magnification and image multiplicity, is indicated by the solid curve. For shallow image surveys with limiting depth brighter than ~ 22 such as the ZTF survey, the magnification approach dominates in providing most of the expected lensed SNe. For deep image surveys with limiting depth fainter than ~ 23 such as the LSST survey, the image multiplicity approach starts to dominate. Figure taken from Wojtak et al. (2019).

stinsky, 2020). The concept is that the temporal series of images will show the multiple SN images appearing at different epochs. Even if the multiple SN images are not well resolved, the centroids of the distribution of light would change as the multiple SN images brighten and dim at different times. Such change in the features of the object helps the neural network to distinguish lensed SN (with multiple SN images) from non-lensed SN (with single SN image). Using simulated images of YSE, Kodi Ramanah et al. (2021) demonstrated that the spatio-temporal network improves the classification accuracy by $\sim 20\%$ compared to networks that use static (e.g., single-epoch) images. The new development spatio-temporal network is very promising for application to the LSST.

4.2 Expected number of lensed SN events

Strongly lensed transients are very rare. Hence, deep, wide-field time-domain optical and Near-IR surveys have the best chances to find samples of lensed SNe. Among these, the (optical) LSST survey at the Vera C. Rubin Observatory to see first light in 2024, and the (NIR) Roman satellite, planned for launch some years later offer the best opportunities. In both cases, between several tens to hundreds of strongly lensed supernovae may be expected throughout the multi-year surveys (Goobar et al., 2002; Oguri and Marshall, 2010; Quimby et al., 2014; Goldstein et al., 2019; Wojtak et al., 2019; Pierel et al., 2021). The cumulative number of SNe, Type Ia and core-collapse, expected to be found every year by LSST as a

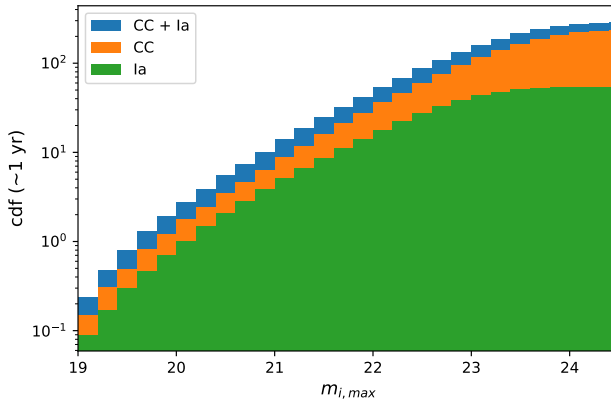


Fig. 17 Cumulative number of lensed Type Ia and core-collapse supernovae detections by the LSST survey per year as a function of their peak i -band magnitude, as computed in Goldstein et al. (2019). Figure credit: Ana Sagués Carracedo.

function of the detection threshold is shown in Fig. 17. A potential concern is the low cadence of the observations, which may require follow-up observations to measure time delays accurately (Huber et al., 2019).

4.3 Expected lens properties

Fig. 18 shows simulations by Goldstein et al. (2019) of the distribution of system properties for strongly lensed SNe Ia in the LSST survey. The typical source redshift is $z_s \sim 0.9$ with time delays between 2 and 3 weeks. With a median image separation close to $1''$ and the expected good seeing conditions at the Rubin Observatory coupled with the plate-scale of the camera, most events would be spatially resolved.

4.4 Requirements on follow-up observations

Full scientific exploitation of strongly lensed SNe depends on 1) early transient detection, ideally well before light curve peak; 2) rapid spectroscopic classification of the transient; 3) well-sampled, spatially resolved light curves; and 4) good wavelength coverage, necessary for accurate extinction corrections. From Fig. 17 one can see that the vast majority of the lensed SNe in forthcoming surveys will have (summed) peak magnitudes fainter than 21 mag. Hence, spectroscopic classification requires 8-m class telescopes, in most cases, potentially a major challenge. As argued in Sec. 3.4, an accurate measurement of the image magnifications requires a wide lever arm in wavelength coverage of the spatially resolved images, for at least a handful of epochs along the light curve. The new space telescope, JWST, would be ideally suited for follow-up. Its Near-IR sensitivity is an excellent match to the source redshifts shown in Fig. 18.

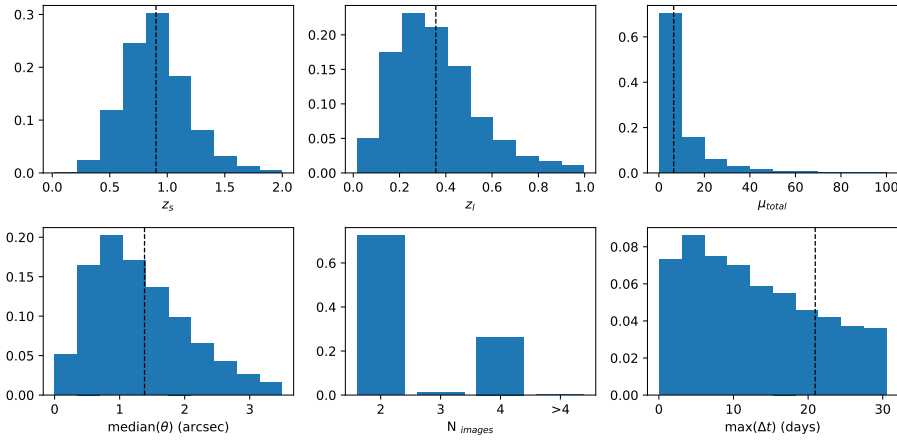


Fig. 18 Predicted system configurations for strongly lensed Type Ia supernovae in LSST as computed in Goldstein et al. (2019). Figure credit: Ana Sagüés Carracedo.

5 Summary

The first discoveries of strongly lensed SNe in recent years are opening a new window of exploration for cosmological and astrophysical studies. In this review, we have provided an overview of the analysis and results from these first lensed SN systems, and the future prospects for this exciting new field. The main takeaway points are as follows.

- There are currently five strongly lensed SN systems with spatially resolved SN images. Three systems are lensed by galaxy clusters and two lensed by individual galaxies.
- Time delays between the multiple SN images of a lensed SN allow direct measurements of (1) the time-delay distance, (2) the angular-diameter distance to the lens in the case where stellar kinematic measurements of the lens galaxy are available, and (3) the luminosity distance in the case of a Type Ia SN that is a standardisable candle, as long as the SN magnifications due to microlensing and millilensing can be accurately accounted for. These distance measurements provide competitive constraints on cosmological parameters, particularly H_0 .
- Several new methods to infer the time delays of lensed SNe have been developed in recent years, employing different kinds of data such as light curves, color curves or spectral evolution of SNe. Time-delay measurements with uncertainties of ~ 1 day are achievable with real and mock data. The fractional uncertainty in the delays contribute directly to the fractional uncertainty on the time-delay distance and the lens angular-diameter distance.
- Cosmographic constraints, especially the Hubble constant inference, from SN Refsdal are forthcoming. We expect that a modest sample of 20 lensed SNe Ia from the upcoming LSST to yield H_0 with nearly 1% precision in flat Λ CDM cosmology.

- The time delays of lensed SNe provide a unique opportunity to acquire very early-phase observations of SNe, especially in the rest-frame UV, and probe SN progenitors.
- Lensing magnifications allow the acquisition of spectra of SN above $z > 1$, that are crucial to reduce systematic uncertainties in SN Ia cosmology.
- Microlensing of SNe provides an avenue to constrain the sizes of the SN at different wavelengths.
- The dust properties in the (foreground lens) galaxies can be measured through the multiple SN sight lines in lensed SN systems.
- Various methods have been developed to search for lensed SNe, through e.g., the monitoring of known lens systems, magnification, image multiplicity, and spatio-temporal evolution in the imaging. Depending on the selection criteria, we expect at least dozens of lensed SNe to explode in the upcoming LSST, with their properties summarized in Section 4.3.

We are entering a new era of lensed SNe with the upcoming wide-field cadenced imaging surveys. Rapid follow-up observations including spectroscopic typing and light curve monitoring, will be crucial and necessary to make the best use of such events for cosmological and astrophysical studies.

Acknowledgements We thank Luke Weisenbach for producing Fig. 5, and Raoul Cañameras and Paul Schechter for discussions and feedback on the manuscript. We are grateful to the International Space Science Institute (ISSI) in Bern for the hospitality and the stimulating workshop on “Strong Gravitational Lensing”. SHS thanks the Max Planck Society for support through the Max Planck Research Group and the Max Planck Fellowship. This project has received funding from the European Research Council (ERC) under the European Union’s Horizon 2020 research and innovation programme (LENSNOVA: grant agreement No 771776). This research is supported in part by the Excellence Cluster ORIGINS which is funded by the Deutsche Forschungsgemeinschaft (DFG, German Research Foundation) under Germany’s Excellence Strategy – EXC-2094 – 390783311. AG acknowledges support from the Swedish National Space Board and *Vetenskapsrådet*, the Swedish Research Council. TEC is funded by a Royal Society University Research Fellowship. GV has received funding from the European Union’s Horizon 2020 research and innovation programme under the Marie Skłodowska-Curie grant agreement No 897124. GV’s research was made possible by the generosity of Eric and Wendy Schmidt by recommendation of the Schmidt Futures program.

References

- R. Amanullah, A. Goobar, B. Clément, J.-G. Cuby, H. Dahle, T. Dahlén, J. Hjorth, S. Fabbro, J. Jönsson, J.-P. Kneib, C. Lidman, M. Limousin, B. Milvang-Jensen, E. Mörtsell, J. Nordin, K. Paech, J. Richard, T. Riehm, V. Stanishev, D. Watson, A Highly Magnified Supernova at $z = 1.703$ behind the Massive Galaxy Cluster A1689. *Astrophys. J. Letters* **742**(1), 7 (2011). doi:10.1088/2041-8205/742/1/L7
- R. Amanullah, J. Johansson, A. Goobar, R. Ferretti, S. Papadogiannakis, T. Petrushevska, P.J. Brown, Y. Cao, C. Contreras, H. Dahle, N. Elias-Rosa, J.P.U. Fynbo, J. Gorosabel, L. Guaita, L. Hangard, D.A. Howell, E.Y. Hsiao, E. Kankare, M. Kasliwal, G. Leloudas, P. Lundqvist, S. Mattila, P. Nugent, M.M. Phillips, A. Sandberg, V. Stanishev, M. Sullivan, F. Taddia, G. Östlin, S. Asadi, R. Herrero-Illana, J.J. Jensen, K. Karhunen, S. Lazarevic, E. Varenius, P. Santos, S.S. Sridhar, S.H.J. Wallström, J. Wiegert, Diversity in extinction laws of

- Type Ia supernovae measured between 0.2 and 2 μm . Mon. Notices of the Royal Astron. Soc. **453**(3), 3300–3328 (2015). doi:10.1093/mnras/stv1505
- M.W. Auger, T. Treu, A.S. Bolton, R. Gavazzi, L.V.E. Koopmans, P.J. Marshall, L.A. Moustakas, S. Burles, The Sloan Lens ACS Survey. X. Stellar, Dynamical, and Total Mass Correlations of Massive Early-type Galaxies. *Astrophys. J.* **724**(1), 511–525 (2010). doi:10.1088/0004-637X/724/1/511
- R. Bacon, M. Accardo, L. Adjali, H. Anwand, S. Bauer, I. Biswas, J. Blaizot, D. Boudon, S. Brau-Nogue, J. Brinchmann, P. Caillier, L. Capoani, C.M. Carollo, T. Contini, P. Couderc, E. Daguisé, S. Deiries, B. Delabre, S. Dreizler, J. Dubois, M. Dupieux, C. Dupuy, E. Emsellem, T. Fechner, A. Fleischmann, M. François, G. Gallou, T. Gharsa, A. Glindemann, D. Gojak, B. Guideroni, G. Hansali, T. Hahn, A. Jarno, A. Kelz, C. Koehler, J. Kosmalski, F. Laurent, M. Le Floch, S.J. Lilly, J.-L. Lizon, M. Loupias, A. Manescau, C. Monstein, H. Nicklas, J.-C. Olaya, L. Pares, L. Pasquini, A. Pécontal-Rousset, R. Pelló, C. Petit, E. Popow, R. Reiss, A. Remillieux, E. Renault, M. Roth, G. Rupprecht, D. Serre, J. Schaye, G. Soucail, M. Steinmetz, O. Streicher, R. Stuik, H. Valentin, J. Vernet, P. Weilbacher, L. Wisotzki, N. Yerle, The MUSE second-generation VLT instrument, in *Ground-based and Airborne Instrumentation for Astronomy III*, ed. by I.S. McLean, S.K. Ramsay, H. Takami Society of Photo-Optical Instrumentation Engineers (SPIE) Conference Series, vol. 7735, 2010, p. 773508. doi:10.1117/12.856027
- H. Bagherpour, D. Branch, R. Kantowski, Effects of Gravitational Microlensing on P Cygni Profiles of Type Ia Supernovae. *Astrophys. J.* **638**(2), 946–950 (2006). doi:10.1086/498889
- M. Barnabè, A.A. Dutton, P.J. Marshall, M.W. Auger, B.J. Brewer, T. Treu, A.S. Bolton, D.C. Koo, L.V.E. Koopmans, The SWELLS survey - IV. Precision measurements of the stellar and dark matter distributions in a spiral lens galaxy. *Mon. Notices of the Royal Astron. Soc.* **423**(2), 1073–1088 (2012). doi:10.1111/j.1365-2966.2012.20934.x
- J. Bayer, S. Huber, C. Vogl, S.H. Suyu, S. Taubenberger, D. Sluse, J.H.H. Chan, W.E. Kerzendorf, HOLISMOKES – V. Microlensing of type II supernovae and time-delay inference through spectroscopic phase retrieval. arXiv e-prints, 2101–06229 (2021)
- E.C. Bellm, S.R. Kulkarni, M.J. Graham, R. Dekany, R.M. Smith, R. Riddle, F.J. Masci, G. Helou, T.A. Prince, S.M. Adams, C. Barbarino, T. Barlow, J. Bauer, R. Beck, J. Belicki, R. Biswas, N. Blagorodnova, D. Bodewits, B. Bolin, V. Brinnel, T. Brooke, B. Bue, M. Bulla, R. Burruss, S.B. Cenko, C.-K. Chang, A. Connolly, M. Coughlin, J. Cromer, V. Cunningham, K. De, A. Delacroix, V. Desai, D.A. Duev, G. Eadie, T.L. Farnham, M. Feeney, U. Feindt, D. Flynn, A. Franckowiak, S. Frederick, C. Fremling, A. Gal-Yam, S. Gezari, M. Giomi, D.A. Goldstein, V.Z. Golkhou, A. Goobar, S. Groom, E. Hacopians, D. Hale, J. Henning, A.Y.Q. Ho, D. Hover, J. Howell, T. Hung, D. Huppenkothen, D. Imel, W.-H. Ip, Ž. Ivezić, E. Jackson, L. Jones, M. Juric, M.M. Kasliwal, S. Kaspi, S. Kaye, M.S.P. Kelley, M. Kowalski, E. Kramer, T. Kupfer, W. Landry, R.R. Laher, C.-D. Lee, H.W. Lin, Z.-Y. Lin, R. Lunnan, M. Giomi, A. Mahabal, P. Mao, A.A. Miller, S. Monkewitz, P. Murphy, C.-C. Ngeow, J. Nordin, P. Nugent, E. Ofek, M.T. Patterson, B. Penprase, M. Porter, L. Rauch, U. Rebbapragada, D. Reiley, M. Rigault, H. Rodriguez, J. van Roestel, B. Rusholme, J. van Santen, S. Schulze, D.L. Shupe, L.P. Singer, M.T. Soumagnac, R. Stein, J. Surace, J.

- Sollerman, P. Szkody, F. Taddia, S. Terek, A. Van Sistine, S. van Velzen, W.T. Vestrand, R. Walters, C. Ward, Q.-Z. Ye, P.-C. Yu, L. Yan, J. Zolkower, The Zwicky Transient Facility: System Overview, Performance, and First Results. *PASP* **131**(995), 018002 (2019). doi:10.1088/1538-3873/aaecbe
- M. Betoule, R. Kessler, J. Guy, J. Mosher, D. Hardin, R. Biswas, P. Astier, P. El-Hage, M. Konig, S. Kuhlmann, J. Marriner, R. Pain, N. Regnault, C. Balland, B.A. Bassett, P.J. Brown, H. Campbell, R.G. Carlberg, F. Cellier-Holzem, D. Cinabro, A. Conley, C.B. D'Andrea, D.L. DePoy, M. Doi, R.S. Ellis, S. Fabbro, A.V. Filippenko, R.J. Foley, J.A. Frieman, D. Fouchez, L. Galbany, A. Goobar, R.R. Gupta, G.J. Hill, R. Hlozek, C.J. Hogan, I.M. Hook, D.A. Howell, S.W. Jha, L. Le Guillou, G. Leloudas, C. Lidman, J.L. Marshall, A. Möller, A.M. Mourão, J. Neveu, R. Nichol, M.D. Olmstead, N. Palanque-Delabrouille, S. Perlmutter, J.L. Prieto, C.J. Pritchett, M. Richmond, A.G. Riess, V. Ruhlmann-Kleider, M. Sako, K. Schahmaneche, D.P. Schneider, M. Smith, J. Sollerman, M. Sullivan, N.A. Walton, C.J. Wheeler, Improved cosmological constraints from a joint analysis of the SDSS-II and SNLS supernova samples. *Astron. Astrophys.* **568**, 22 (2014). doi:10.1051/0004-6361/201423413
- S. Birrer, A.J. Shajib, A. Galan, M. Millon, T. Treu, A. Agnello, M. Auger, G.C.-F. Chen, L. Christensen, T. Collett, F. Courbin, C.D. Fassnacht, L.V.E. Koopmans, P.J. Marshall, J.-W. Park, C.E. Rusu, D. Sluse, C. Spiniello, S.H. Suyu, S. Wagner-Carena, K.C. Wong, M. Barnabè, A.S. Bolton, O. Czoske, X. Ding, J.A. Frieman, L. Van de Vyvere, TDCOSMO. IV. Hierarchical time-delay cosmography – joint inference of the Hubble constant and galaxy density profiles. *Astron. Astrophys.* **643**, 165 (2020). doi:10.1051/0004-6361/202038861
- S. Birrer, M. Millon, D. Sluse, A.J. Shajib, F. Courbin, L.V.E. Koopmans, S.H. Suyu, T. Treu, Time-Delay Cosmography: Measuring the Hubble Constant and other cosmological parameters with strong gravitational lensing. arXiv e-prints, 2210–10833 (2022)
- S. Birrer, S. Dhawan, A.J. Shajib, The Hubble constant from strongly lensed supernovae with standardizable magnifications. arXiv e-prints, 2107–12385 (2021)
- J.S. Bloom, D. Kasen, K.J. Shen, P.E. Nugent, N.R. Butler, M.L. Graham, D.A. Howell, U. Kolb, S. Holmes, C.A. Haswell, V. Burwitz, J. Rodriguez, M. Sullivan, A Compact Degenerate Primary-star Progenitor of SN 2011fe. *Astrophys. J. Letters* **744**(2), 17 (2012). doi:10.1088/2041-8205/744/2/L17
- A.S. Bolton, S. Burles, L.V.E. Koopmans, T. Treu, L.A. Moustakas, The Sloan Lens ACS Survey. I. A Large Spectroscopically Selected Sample of Massive Early-Type Lens Galaxies. *Astrophys. J.* **638**(2), 703–724 (2006). doi:10.1086/498884
- A.S. Bolton, S. Burles, L.V.E. Koopmans, T. Treu, R. Gavazzi, L.A. Moustakas, R. Wayth, D.J. Schlegel, The Sloan Lens ACS Survey. V. The Full ACS Strong-Lens Sample. *Astrophys. J.* **682**(2), 964–984 (2008). doi:10.1086/589327
- A.S. Bolton, J.R. Brownstein, C.S. Kochanek, Y. Shu, D.J. Schlegel, D.J. Eisenstein, D.A. Wake, N. Connolly, C. Maraston, R.A. Arneson, B.A. Weaver, The BOSS Emission-Line Lens Survey. II. Investigating Mass-density Profile Evolution in the SLACS+BELLS Strong Gravitational Lens Sample. *Astrophys. J.* **757**(1), 82 (2012). doi:10.1088/0004-637X/757/1/82
- J.R. Brownstein, A.S. Bolton, D.J. Schlegel, D.J. Eisenstein, C.S. Kochanek, N. Connolly, C. Maraston, P. Pandey, S. Seitz, D.A. Wake, W.M. Wood-Vasey, J. Brinkmann, D.P. Schneider, B.A. Weaver, The BOSS Emission-Line Lens Survey

- (BELLS). I. A Large Spectroscopically Selected Sample of Lens Galaxies at Redshift ~ 0.5 . *Astrophys. J.* **744**(1), 41 (2012). doi:10.1088/0004-637X/744/1/41
- M. Bulla, A.A. Miller, Y. Yao, L. Dessart, S. Dhawan, S. Papadogiannakis, R. Biswas, A. Goobar, S.R. Kulkarni, J. Nordin, P. Nugent, A. Polin, J. Sollerman, E.C. Bellm, M.W. Coughlin, R. Dekany, V.Z. Golkhou, M.J. Graham, M.M. Kasliwal, T. Kupfer, R.R. Laher, F.J. Masci, M. Porter, B. Rusholme, D.L. Shupe, ZTF Early Observations of Type Ia Supernovae III: Early-Time Colors as a Test for Explosion Models and Multiple Populations. arXiv e-prints, 2001–00587 (2020)
- R. Cañameras, N.P.H. Nesvadba, D. Guery, T. McKenzie, S. König, G. Petipas, H. Dole, B. Frye, I. Flores-Cacho, L. Montier, M. Negrello, A. Beelen, F. Boone, D. Dicken, G. Lagache, E. Le Floc'h, B. Altieri, M. Béthermin, R. Chary, G. de Zotti, M. Giard, R. Kneissl, M. Krips, S. Malhotra, C. Martinache, A. Omont, E. Pointecouteau, J.-L. Puget, D. Scott, G. Soucail, I. Valtchanov, N. Welikala, L. Yan, Planck's dusty GEMS: The brightest gravitationally lensed galaxies discovered with the Planck all-sky survey. *Astron. Astrophys.* **581**, 105 (2015). doi:10.1051/0004-6361/201425128
- R. Cañameras, S. Schuldt, S.H. Suyu, S. Taubenberger, T. Meinhardt, L. Leal-Taixé, C. Lemon, K. Rojas, E. Savary, HOLISMOKEs. II. Identifying galaxy-scale strong gravitational lenses in Pan-STARRS using convolutional neural networks. *Astron. Astrophys.* **644**, 163 (2020). doi:10.1051/0004-6361/202038219
- R. Cañameras, S. Schuldt, Y. Shu, S.H. Suyu, S. Taubenberger, T. Meinhardt, L. Leal-Taixé, D.C.-Y. Chao, K.T. Inoue, A.T. Jaelani, A. More, HOLISMOKEs – VI. New galaxy-scale strong lens candidates from the HSC-SSP imaging survey. arXiv e-prints, 2107–07829 (2021)
- W. Chen, P.L. Kelly, M. Oguri, T.J. Broadhurst, J.M. Diego, N. Emami, A.V. Filippenko, T.L. Treu, A. Zitrin, Shock cooling of a red-supergiant supernova at redshift 3 in lensed images. *Nature* **611**(7935), 256–259 (2022). doi:10.1038/s41586-022-05252-5
- G. Chirivi, A. Yıldırım, S.H. Suyu, A. Halkola, Gravitational Lensing and Dynamics (GLaD): combined analysis to unveil properties of high-redshift galaxies. *Astron. Astrophys.* **643**, 135 (2020). doi:10.1051/0004-6361/202037929
- R. Chornock, E. Berger, A. Rest, D. Milisavljevic, R. Lunnan, R.J. Foley, A.M. Soderberg, S.J. Smartt, A.J. Burgasser, P. Challis, L. Chomiuk, I. Czekala, M. Drout, W. Fong, M.E. Huber, R.P. Kirshner, C. Leibler, B. McLeod, G.H. Marion, G. Narayan, A.G. Riess, K.C. Roth, N.E. Sanders, D. Scolnic, K. Smith, C.W. Stubbs, J.L. Tonry, S. Valenti, W.S. Burgett, K.C. Chambers, K.W. Hodapp, N. Kaiser, R.-P. Kudritzki, E.A. Magnier, P.A. Price, PS1-10afx at $z = 1.388$: Pan-STARRS1 Discovery of a New Type of Superluminous Supernova. *Astrophys. J.* **767**(2), 162 (2013). doi:10.1088/0004-637X/767/2/162
- F. Courbin, V. Bonvin, E. Buckley-Geer, C.D. Fassnacht, J. Frieman, H. Lin, P.J. Marshall, S.H. Suyu, T. Treu, T. Anguita, V. Motta, G. Meylan, E. Paic, M. Tewes, A. Agnello, D.C.-Y. Chao, M. Chijani, D. Gilman, K. Rojas, P. Williams, A. Hempel, S. Kim, R. Lachapelle, M. Rabus, T.M.C. Abbott, S. Allam, J. Annis, M. Banerji, K. Bechtol, A. Benoit-Lévy, D. Brooks, D.L. Burke, A. Carnero Rosell, M. Carrasco Kind, J. Carretero, C.B. D'Andrea, L.N. da Costa, C. Davis, D.L. DePoy, S. Desai, B. Flaugher, P. Fosalba, J. García-Bellido, E. Gaztanaga, D.A. Goldstein, D. Gruen, R.A. Gruendl, J. Gschwend, G. Gutierrez, K. Honscheid, D.J. James, K. Kuehn, S. Kuhlmann, N. Kuropatkin, O. Lahav, M. Lima,

- M.A.G. Maia, M. March, J.L. Marshall, R.G. McMahon, F. Menanteau, R. Miquel, B. Nord, A.A. Plazas, E. Sanchez, V. Scarpine, R. Schindler, M. Schubnell, I. Sevilla-Noarbe, M. Smith, M. Soares-Santos, F. Sobreira, E. Suchyta, G. Tarle, D.L. Tucker, A.R. Walker, W. Wester, COSMOGRAIL: the COsmological MOnitoring of GRAvItational Lenses. XVI. Time delays for the quadruply imaged quasar DES J0408-5354 with high-cadence photometric monitoring. *Astron. Astrophys.* **609**, 71 (2018). doi:10.1051/0004-6361/201731461
- P. Craig, K. O'Connor, S. Chakrabarti, S.A. Rodney, J.R. Pierel, C. McCully, I. Perez-Fournon, A targeted search for strongly lensed supernovae and expectations for targeted searches in the Rubin era. arXiv e-prints, 2111-01680 (2021)
- S. Dhawan, J. Johansson, A. Goobar, R. Amanullah, E. Mörtsell, S.B. Cenko, A. Cooray, O. Fox, D. Goldstein, R. Kalender, M. Kasliwal, S.R. Kulkarni, W.H. Lee, H. Nayyeri, P. Nugent, E. Ofek, R. Quimby, Magnification, dust, and time-delay constraints from the first resolved strongly lensed Type Ia supernova iPTF16geu. *Mon. Notices of the Royal Astron. Soc.* **491**(2), 2639–2654 (2020). doi:10.1093/mnras/stz2965
- E. Di Valentino, O. Mena, S. Pan, L. Visinelli, W. Yang, A. Melchiorri, D.F. Mota, A.G. Riess, J. Silk, In the realm of the Hubble tension-a review of solutions. *Classical and Quantum Gravity* **38**(15), 153001 (2021). doi:10.1088/1361-6382/ac086d
- J.M. Diego, G. Bernstein, W. Chen, A. Goobar, J.P. Johansson, P.L. Kelly, E. Mörtsell, J.W. Nightingale, Microlensing and the type Ia supernova iPTF16geu. *Astron. Astrophys.* **662**, 34 (2022). doi:10.1051/0004-6361/202143009
- X. Ding, K. Liao, S. Birrer, A.J. Shajib, T. Treu, L. Yang, Improved time-delay lens modelling and H_0 inference with transient sources. *Mon. Notices of the Royal Astron. Soc.* **504**(4), 5621–5628 (2021). doi:10.1093/mnras/stab1240
- G. Dobler, C.R. Keeton, Microlensing of Lensed Supernovae. *Astrophys. J.* **653**(2), 1391–1399 (2006). doi:10.1086/508769
- A. Einstein, Lens-Like Action of a Star by the Deviation of Light in the Gravitational Field. *Science* **84**(2188), 506–507 (1936). doi:10.1126/science.84.2188.506
- Á. Elíasdóttir, J. Hjorth, S. Toft, I. Burud, D. Paraficz, Extinction Curves of Lensing Galaxies out to $z = 1$. *Astrophys. J. Supplement* **166**(2), 443–469 (2006). doi:10.1086/507131
- E.E. Falco, M.V. Gorenstein, I.I. Shapiro, On model-dependent bounds on H_0 from gravitational images : application to Q 0957+561 A, B. *Astrophys. J. Letters* **289**, 1–4 (1985). doi:10.1086/184422
- E.E. Falco, C.D. Impey, C.S. Kochanek, J. Lehár, B.A. McLeod, H.-W. Rix, C.R. Keeton, J.A. Muñoz, C.Y. Peng, Dust and Extinction Curves in Galaxies with $z > 0$: The Interstellar Medium of Gravitational Lens Galaxies. *Astrophys. J.* **523**(2), 617–632 (1999). doi:10.1086/307758
- C.D. Fassnacht, E. Xanthopoulos, L.V.E. Koopmans, D. Rusin, A Determination of H_0 with the CLASS Gravitational Lens B1608+656. III. A Significant Improvement in the Precision of the Time Delay Measurements. *Astrophys. J.* **581**(2), 823–835 (2002). doi:10.1086/344368
- M.M. Fausnaugh, P.J. Valley, C.S. Kochanek, B.J. Shappee, K.Z. Stanek, M.A. Tucker, G.R. Ricker, R. Vanderspek, D.W. Latham, S. Seager, J.N. Winn, J.M. Jenkins, T. Daylan, J.P. Doty, G. Furesz, A.M. Levine, R. Morris, A. Pal, L. Sha, E.B. Ting, B. Wohler, Early Time Light Curves of 18 Bright Type Ia Supernovae Observed with TESS. arXiv e-prints, 1904-02171 (2019)

- M. Fink, W. Hillebrandt, F.K. Röpke, Double-detonation supernovae of sub-Chandrasekhar mass white dwarfs. *Astron. Astrophys.* **476**(3), 1133–1143 (2007). doi:10.1051/0004-6361:20078438
- M. Foxley-Marrable, T.E. Collett, G. Vernardos, D.A. Goldstein, D. Bacon, The impact of microlensing on the standardization of strongly lensed Type Ia supernovae. *Mon. Notices of the Royal Astron. Soc.* **478**(4), 5081–5090 (2018). doi:10.1093/mnras/sty1346
- M. Foxley-Marrable, T.E. Collett, C. Frohmaier, D.A. Goldstein, D. Kasen, E. Swann, D. Bacon, Observing the earliest moments of supernovae using strong gravitational lenses. *Mon. Notices of the Royal Astron. Soc.* **495**(4), 4622–4637 (2020). doi:10.1093/mnras/staa1289
- R. Gavazzi, T. Treu, P.J. Marshall, F. Brault, A. Ruff, The SL2S Galaxy-scale Gravitational Lens Sample. I. The Alignment of Mass and Light in Massive Early-type Galaxies at $z = 0.2\text{--}0.9$. *Astrophys. J.* **761**(2), 170 (2012). doi:10.1088/0004-637X/761/2/170
- D.A. Goldstein, P.E. Nugent, How to Find Gravitationally Lensed Type Ia Supernovae. *Astrophys. J. Letters* **834**(1), 5 (2017). doi:10.3847/2041-8213/834/1/L5
- D.A. Goldstein, P.E. Nugent, A. Goobar, Rates and Properties of Supernovae Strongly Gravitationally Lensed by Elliptical Galaxies in Time-domain Imaging Surveys. *Astrophys. J. Supplement* **243**(1), 6 (2019). doi:10.3847/1538-4365/ab1fe0
- D.A. Goldstein, P.E. Nugent, D.N. Kasen, T.E. Collett, Precise Time Delays from Strongly Gravitationally Lensed Type Ia Supernovae with Chromatically Microlensed Images. *Astrophys. J.* **855**(1), 22 (2018). doi:10.3847/1538-4357/aaa975
- S. González-Gaitán, N. Tominaga, J. Molina, L. Galbany, F. Bufano, J.P. Anderson, C. Gutierrez, F. Förster, G. Pignata, M. Bersten, D.A. Howell, M. Sullivan, R. Carlberg, T. de Jaeger, M. Hamuy, P.V. Baklanov, S.I. Blinnikov, The rise-time of Type II supernovae. *Mon. Notices of the Royal Astron. Soc.* **451**(2), 2212–2229 (2015). doi:10.1093/mnras/stv1097
- J.I. González Hernández, P. Ruiz-Lapuente, H.M. Tabernero, D. Montes, R. Canal, J. Méndez, L.R. Bedin, No surviving evolved companions of the progenitor of SN 1006. *Nature* **489**(7417), 533–536 (2012). doi:10.1038/nature11447
- A. Goobar, E. Mörtsell, R. Amanullah, P. Nugent, Cosmological parameters from lensed supernovae. *Astron. Astrophys.* **393**, 25–32 (2002). doi:10.1051/0004-6361:20020987
- A. Goobar, K. Paech, V. Stanishev, R. Amanullah, T. Dahlén, J. Jönsson, J.P. Kneib, C. Lidman, M. Limousin, E. Mörtsell, S. Nobili, J. Richard, T. Riehm, M. von Strauss, Near-IR search for lensed supernovae behind galaxy clusters. II. First detection and future prospects. *Astron. Astrophys.* **507**(1), 71–83 (2009). doi:10.1051/0004-6361/200811254
- A. Goobar, M. Kromer, R. Siverd, K.G. Stassun, J. Pepper, R. Amanullah, M. Kasliwal, J. Sollerman, F. Taddia, Constraints on the Origin of the First Light from SN 2014J. *Astrophys. J.* **799**(1), 106 (2015). doi:10.1088/0004-637X/799/1/106
- A. Goobar, R. Amanullah, S.R. Kulkarni, P.E. Nugent, J. Johansson, C. Steidel, D. Law, E. Mörtsell, R. Quimby, N. Blagorodnova, A. Brandeker, Y. Cao, A. Cooray, R. Ferretti, C. Fremling, L. Hangard, M. Kasliwal, T. Kupfer, R. Lunnan, F. Masci, A.A. Miller, H. Nayyeri, J.D. Neill, E.O. Ofek, S. Papado-

- giannakis, T. Petrushevska, V. Ravi, J. Sollerman, M. Sullivan, F. Taddia, R. Walters, D. Wilson, L. Yan, O. Yaron, iPTF16geu: A multiply imaged, gravitationally lensed type Ia supernova. *Science* **356**(6335), 291–295 (2017). doi:10.1126/science.aal2729
- A. Goobar, J. Johansson, S. Schulze, N. Arendse, A. Sagués Carracedo, S. Dhawan, E. Mörtsell, C. Fremling, L. Yan, D. Perley, J. Sollerman, R. Joseph, K.-R. Hinds, W. Meynardie, I. Andreoni, E. Bellm, J. Bloom, T.E. Collett, A. Drake, M. Graham, M. Kasliwal, S. Kulkarni, A. Miller, J.D. Neill, J. Nordin, J. Pierel, J. Richard, R. Riddle, M. Rigault, B. Rusholme, Y. Sharma, R. Stein, G. Stewart, A. Townsend, J. Vinko, J.C. Wheeler, A. Wold, SN Zwicky: uncovering a population of gravitational lens galaxies with magnified “standard candles”. arXiv e-prints, 2211–00656 (2022)
- C. Grillo, W. Karman, S.H. Suyu, P. Rosati, I. Balestra, A. Mercurio, M. Lombardi, T. Treu, G.B. Caminha, A. Halkola, S.A. Rodney, R. Gavazzi, K.I. Caputi, The Story of Supernova “Refsdal” Told by Muse. *Astrophys. J.* **822**(2), 78 (2016). doi:10.3847/0004-637X/822/2/78
- C. Grillo, P. Rosati, S.H. Suyu, I. Balestra, G.B. Caminha, A. Halkola, P.L. Kelly, M. Lombardi, A. Mercurio, S.A. Rodney, T. Treu, Measuring the Value of the Hubble Constant “à la Refsdal”. *Astrophys. J.* **860**(2), 94 (2018). doi:10.3847/1538-4357/aac2c9
- C. Grillo, P. Rosati, S.H. Suyu, G.B. Caminha, A. Mercurio, A. Halkola, On the Accuracy of Time-delay Cosmography in the Frontier Fields Cluster MACS J1149.5+2223 with Supernova Refsdal. *Astrophys. J.* **898**(1), 87 (2020). doi:10.3847/1538-4357/ab9a4c
- C. Gunnarsson, A. Goobar, Massive galaxy clusters as gravitational telescopes for distant supernovae. *Astron. Astrophys.* **405**, 859–866 (2003). doi:10.1051/0004-6361:20030648
- J. Hjorth, P.M. Vreeswijk, C. Gall, D. Watson, On Inferring Extinction Laws in $z \sim 6$ Quasars as Signatures of Supernova Dust. *Astrophys. J.* **768**(2), 173 (2013). doi:10.1088/0004-637X/768/2/173
- X. Huang, C. Storfer, V. Ravi, A. Pilon, M. Domingo, D.J. Schlegel, S. Bailey, A. Dey, R.R. Gupta, D. Herrera, S. Juneau, M. Landriau, D. Lang, A. Meisner, J. Moustakas, A.D. Myers, E.F. Schlafly, F. Valdes, B.A. Weaver, J. Yang, C. Yèche, Finding Strong Gravitational Lenses in the DESI DECam Legacy Survey. *Astrophys. J.* **894**(1), 78 (2020). doi:10.3847/1538-4357/ab7ffb
- X. Huang, C. Storfer, A. Gu, V. Ravi, A. Pilon, W. Sheu, R. Venguswamy, S. Banka, A. Dey, M. Landriau, D. Lang, A. Meisner, J. Moustakas, A.D. Myers, R. Sajith, E.F. Schlafly, D.J. Schlegel, Discovering New Strong Gravitational Lenses in the DESI Legacy Imaging Surveys. *Astrophys. J.* **909**(1), 27 (2021). doi:10.3847/1538-4357/abd62b
- S. Huber, S.H. Suyu, U.M. Noebauer, V. Bonvin, D. Rothchild, J.H.H. Chan, H. Awan, F. Courbin, M. Kromer, P. Marshall, M. Oguri, T. Ribeiro, LSST Dark Energy Science Collaboration, Strongly lensed SNe Ia in the era of LSST: observing cadence for lens discoveries and time-delay measurements. *Astron. Astrophys.* **631**, 161 (2019). doi:10.1051/0004-6361/201935370
- S. Huber, S.H. Suyu, D. Ghoshdastidar, S. Taubenberger, V. Bonvin, J.H.H. Chan, M. Kromer, U.M. Noebauer, S.A. Sim, L. Leal-Taixé, HOLISMOKES - VII. Time-delay measurement of strongly lensed SNe Ia using machine learning. arXiv e-prints, 2108–02789 (2021a)

- S. Huber, S.H. Suyu, U.M. Noebauer, J.H.H. Chan, M. Kromer, S.A. Sim, D. Sluse, S. Taubenberger, HOLISMOKES. III. Achromatic phase of strongly lensed Type Ia supernovae. *Astron. Astrophys.* **646**, 110 (2021b). doi:10.1051/0004-6361/202039218
- I. Iben Jr., A.V. Tutukov, Supernovae of type I as end products of the evolution of binaries with components of moderate initial mass (M not greater than about 9 solar masses). *Astrophys. J. Supplement* **54**, 335–372 (1984). doi:10.1086/190932
- C. Jacobs, K. Glazebrook, T. Collett, A. More, C. McCarthy, Finding strong lenses in CFHTLS using convolutional neural networks. *Mon. Notices of the Royal Astron. Soc.* **471**(1), 167–181 (2017). doi:10.1093/mnras/stx1492
- C. Jacobs, T. Collett, K. Glazebrook, E. Buckley-Geer, H.T. Diehl, H. Lin, C. McCarthy, A.K. Qin, C. Odden, M. Caso Escudero, P. Dial, V.J. Yung, S. Gaitsch, A. Pellico, K.A. Lindgren, T.M.C. Abbott, J. Annis, S. Avila, D. Brooks, D.L. Burke, A. Carnero Rosell, M. Carrasco Kind, J. Carretero, L.N. da Costa, J. De Vicente, P. Fosalba, J. Frieman, J. García-Bellido, E. Gaztanaga, D.A. Goldstein, D. Gruen, R.A. Gruendl, J. Gschwend, D.L. Hollowood, K. Honscheid, B. Hoyle, D.J. James, E. Krause, N. Kuropatkin, O. Lahav, M. Lima, M.A.G. Maia, J.L. Marshall, R. Miquel, A.A. Plazas, A. Roodman, E. Sanchez, V. Scarpine, S. Serrano, I. Sevilla-Noarbe, M. Smith, F. Sobreira, E. Suchyta, M.E.C. Swanson, G. Tarle, V. Vikram, A.R. Walker, Y. Zhang, DES Collaboration, An Extended Catalog of Galaxy-Galaxy Strong Gravitational Lenses Discovered in DES Using Convolutional Neural Networks. *Astrophys. J. Supplement* **243**(1), 17 (2019). doi:10.3847/1538-4365/ab26b6
- M. Jauzac, J. Richard, M. Limousin, K. Knowles, G. Mahler, G.P. Smith, J.-P. Kneib, E. Jullo, P. Natarajan, H. Ebeling, H. Atek, B. Clément, D. Eckert, E. Egami, R. Massey, M. Rexroth, Hubble Frontier Fields: predictions for the return of SN Refsdal with the MUSE and GMOS spectrographs. *Mon. Notices of the Royal Astron. Soc.* **457**(2), 2029–2042 (2016). doi:10.1093/mnras/stw069
- I. Jee, E. Komatsu, S.H. Suyu, Measuring angular diameter distances of strong gravitational lenses. *Journal of Cosmology and Astroparticle Physics* **2015**(11), 033 (2015). doi:10.1088/1475-7516/2015/11/033
- I. Jee, E. Komatsu, S.H. Suyu, D. Huterer, Time-delay cosmography: increased leverage with angular diameter distances. *Journal of Cosmology and Astroparticle Physics* **2016**(4), 031 (2016). doi:10.1088/1475-7516/2016/04/031
- I. Jee, S.H. Suyu, E. Komatsu, C.D. Fassnacht, S. Hilbert, L.V.E. Koopmans, A measurement of the Hubble constant from angular diameter distances to two gravitational lenses. *Science* **365**(6458), 1134–1138 (2019). doi:10.1126/science.aat7371
- J. Johansson, A. Goobar, S.H. Price, A. Sagués Carracedo, L. Della Bruna, P.E. Nugent, S. Dhawan, E. Mörtsell, S. Papadogiannakis, R. Amanullah, D. Goldstein, S.B. Cenko, K. De, A. Dugas, M.M. Kasliwal, S.R. Kulkarni, R. Lunnan, Spectroscopy of the first resolved strongly lensed Type Ia supernova iPTF16geu. *Mon. Notices of the Royal Astron. Soc.* **502**(1), 510–520 (2021). doi:10.1093/mnras/staa3829
- D.O. Jones, R.J. Foley, G. Narayan, J. Hjorth, M.E. Huber, P.D. Aleo, K.D. Alexander, C.R. Angus, K. Auchettl, V.F. Baldassare, S.H. Bruun, K.C. Chambers, D. Chatterjee, D.L. Coppejans, D.A. Coulter, L. DeMarchi, G. Dimitriadis, M.R. Drout, A. Engel, K.D. French, A. Gagliano, C. Gall, T. Hung, L. Izzo, W.V.

- Jacobson-Galán, C.D. Kilpatrick, H. Korhonen, R. Margutti, S.I. Raimundo, E. Ramirez-Ruiz, A. Rest, C. Rojas-Bravo, M.R. Siebert, S.J. Smartt, K.W. Smith, G. Terreran, Q. Wang, R. Wojtak, A. Agnello, Z. Ansari, N. Arendse, A. Baldeschi, P.K. Blanchard, D. Brethauer, J.S. Bright, J.S. Brown, T.J.L. de Boer, S.A. Dodd, J.R. Fairlamb, C. Grillo, A. Hajela, C. Hede, A.N. Kolborg, J.A.P. Law-Smith, C.-C. Lin, E.A. Magnier, K. Malanchev, D. Matthews, B. Mockler, D. Muthukrishna, Y.-C. Pan, H. Pfister, D.K. Ramanah, S. Rest, A. Sarangi, S.L. Schröder, C. Stauffer, M.C. Stroh, K.L. Taggart, S. Tinyanont, R.J. Wainscoat, Young Supernova Experiment, The Young Supernova Experiment: Survey Goals, Overview, and Operations. *Astrophys. J.* **908**(2), 143 (2021). doi:10.3847/1538-4357/abd7f5
- D. Kasen, Seeing the Collision of a Supernova with Its Companion Star. *Astrophys. J.* **708**(2), 1025–1031 (2010). doi:10.1088/0004-637X/708/2/1025
- R. Kawamata, M. Oguri, M. Ishigaki, K. Shimasaku, M. Ouchi, Precise Strong Lensing Mass Modeling of Four Hubble Frontier Field Clusters and a Sample of Magnified High-redshift Galaxies. *Astrophys. J.* **819**(2), 114 (2016). doi:10.3847/0004-637X/819/2/114
- P.L. Kelly, S.A. Rodney, T. Treu, L.-G. Strolger, R.J. Foley, S.W. Jha, J. Selsing, G. Brammer, M. Bradač, S.B. Cenko, O. Graur, A.V. Filippenko, J. Hjorth, C. McCully, A. Molino, M. Nonino, A.G. Riess, K.B. Schmidt, B. Tucker, A. von der Linden, B.J. Weiner, A. Zitrin, Deja Vu All Over Again: The Reappearance of Supernova Refsdal. *Astrophys. J. Letters* **819**(1), 8 (2016a). doi:10.3847/2041-8205/819/1/L8
- P.L. Kelly, G. Brammer, J. Selsing, R.J. Foley, J. Hjorth, S.A. Rodney, L. Christensen, L.-G. Strolger, A.V. Filippenko, T. Treu, C.C. Steidel, A. Strom, A.G. Riess, A. Zitrin, K.B. Schmidt, M. Bradač, S.W. Jha, M.L. Graham, C. McCully, O. Graur, B.J. Weiner, J.M. Silverman, F. Taddia, SN Refsdal: Classification as a Luminous and Blue SN 1987A-like Type II Supernova. *Astrophys. J.* **831**(2), 205 (2016b). doi:10.3847/0004-637X/831/2/205
- P.L. Kelly, S.A. Rodney, T. Treu, R.J. Foley, G. Brammer, K.B. Schmidt, A. Zitrin, A. Sonnenfeld, L.-G. Strolger, O. Graur, A.V. Filippenko, S.W. Jha, A.G. Riess, M. Bradac, B.J. Weiner, D. Scolnic, M.A. Malkan, A. von der Linden, M. Trenti, J. Hjorth, R. Gavazzi, A. Fontana, J.C. Merten, C. McCully, T. Jones, M. Postman, A. Dressler, B. Patel, S.B. Cenko, M.L. Graham, B.E. Tucker, Multiple images of a highly magnified supernova formed by an early-type cluster galaxy lens. *Science* **347**(6226), 1123–1126 (2015). doi:10.1126/science.aaa3350
- W.E. Kerzendorf, S.A. Sim, A spectral synthesis code for rapid modelling of supernovae. *Mon. Notices of the Royal Astron. Soc.* **440**(1), 387–404 (2014). doi:10.1093/mnras/stu055
- C.S. Kochanek, The physics of flash (supernova) spectroscopy. *Mon. Notices of the Royal Astron. Soc.* **483**(3), 3762–3772 (2019). doi:10.1093/mnras/sty3363
- D. Kodi Ramanah, N. Arendse, R. Wojtak, AI-driven spatio-temporal engine for finding gravitationally lensed supernovae. arXiv e-prints, 2107–12399 (2021)
- T.S. Kolatt, M. Bartelmann, Gravitational lensing of type IA supernovae by galaxy clusters. *Mon. Notices of the Royal Astron. Soc.* **296**(3), 763–772 (1998). doi:10.1046/j.1365-8711.1998.01466.x
- I. Kovner, B. Paczynski, Supernovae in Luminous Arcs. *Astrophys. J. Letters* **335**, 9 (1988). doi:10.1086/185328
- F. Lanusse, Q. Ma, N. Li, T.E. Collett, C.-L. Li, S. Ravanbakhsh, R. Mandelbaum,

- B. Póczos, CMU DeepLens: deep learning for automatic image-based galaxy-galaxy strong lens finding. *Mon. Notices of the Royal Astron. Soc.* **473**(3), 3895–3906 (2018). doi:10.1093/mnras/stx1665
- C.-H. Lee, T. Matheson, A. Saha, G. Narayan, M. Soraisam, C. Stubens, N. Wolf, R. Snodgrass, J. Kececioglu, C. Scheidegger, ANTARES: a gateway to ZTF and LSST alerts, in *Society of Photo-Optical Instrumentation Engineers (SPIE) Conference Series*. Society of Photo-Optical Instrumentation Engineers (SPIE) Conference Series, vol. 11449, 2020, p. 1144923. doi:10.1117/12.2560698
- K. Liao, M. Biesiada, Z.-H. Zhu, Strongly Lensed Transient Sources: A Review. *Chinese Physics Letters* **39**(11), 119801 (2022). doi:10.1088/0256-307X/39/11/119801
- M. Limousin, R. Cabanac, R. Gavazzi, J.-P. Kneib, V. Motta, J. Richard, K. Thanjavur, G. Foex, R. Pello, D. Crampton, C. Faure, B. Fort, E. Jullo, P. Marshall, Y. Mellier, A. More, G. Soucail, S. Suyu, M. Swinbank, J.-F. Sygnat, H. Tu, D. Valls-Gabaud, T. Verdugo, J. Willis, A new window of exploration in the mass spectrum: strong lensing by galaxy groups in the SL2S. *Astron. Astrophys.* **502**(2), 445–456 (2009). doi:10.1051/0004-6361/200811473
- M. Livio, P. Mazzali, On the progenitors of Type Ia supernovae. *Physics Reports* **736**, 1–23 (2018). doi:10.1016/j.physrep.2018.02.002
- LSST Science Collaboration, P.A. Abell, J. Allison, S.F. Anderson, J.R. Andrew, J.R.P. Angel, L. Armus, D. Arnett, S.J. Asztalos, T.S. Axelrod, S. Bailey, D.R. Ballantyne, J.R. Bankert, W.A. Barkhouse, J.D. Barr, L.F. Barrientos, A.J. Barth, J.G. Bartlett, A.C. Becker, J. Becla, T.C. Beers, J.P. Bernstein, R. Biswas, M.R. Blanton, J.S. Bloom, J.J. Bochanski, P. Boeshaar, K.D. Borne, M. Bradac, W.N. Brandt, C.R. Bridge, M.E. Brown, R.J. Brunner, J.S. Bullock, A.J. Burgasser, J.H. Burge, D.L. Burke, P.A. Cargile, S. Chandrasekharan, G. Chartas, S.R. Chesley, Y.-H. Chu, D. Cinabro, M.W. Claire, C.F. Claver, D. Clowe, A.J. Connolly, K.H. Cook, J. Cooke, A. Cooray, K.R. Covey, C.S. Culliton, R. de Jong, W.H. de Vries, V.P. Debattista, F. Delgado, I.P. Dell'Antonio, S. Dhital, R. Di Stefano, M. Dickinson, B. Dilday, S.G. Djorgovski, G. Dobler, C. Donalek, G. Dubois-Felsmann, J. Durech, A. Eliasdottir, M. Eracleous, L. Eyer, E.E. Falco, X. Fan, C.D. Fassnacht, H.C. Ferguson, Y.R. Fernandez, B.D. Fields, D. Finkbeiner, E.E. Figueroa, D.B. Fox, H. Francke, J.S. Frank, J. Frieman, S. Fromenteau, M. Furqan, G. Galaz, A. Gal-Yam, P. Garnavich, E. Gawiser, J. Geary, P. Gee, R.R. Gibson, K. Gilmore, E.A. Grace, R.F. Green, W.J. Gressler, C.J. Grillmair, S. Habib, J.S. Haggerty, M. Hamuy, A.W. Harris, S.L. Hawley, A.F. Heavens, L. Hebb, T.J. Henry, E. Hileman, E.J. Hilton, K. Hoadley, J.B. Holberg, M.J. Holman, S.B. Howell, L. Infante, Z. Ivezić, S.H. Jacoby, B. Jain, R. Jedicke, M.J. Jee, J. Garrett Jernigan, S.W. Jha, K.V. Johnston, R.L. Jones, M. Juric, M. Kaasalainen, Stylianis, Kafka, S.M. Kahn, N.A. Kaib, J. Kalirai, J. Kantor, M.M. Kasliwal, C.R. Keeton, R. Kessler, Z. Knezevic, A. Kowalski, V.L. Krabbendam, K.S. Krughoff, S. Kulkarni, S. Kuhlman, M. Lacy, S. Lepine, M. Liang, A. Lien, P. Lira, K.S. Long, S. Lorenz, J.M. Lotz, R.H. Lupton, J. Lutz, L.M. Macri, A.A. Mahabal, R. Mandelbaum, P. Marshall, M. May, P.M. McGehee, B.T. Meadows, A. Meert, A. Milani, C.J. Miller, M. Miller, D. Mills, D. Minniti, D. Monet, A.S. Mukadam, E. Nakar, D.R. Neill, J.A. Newman, S. Nikolaev, M. Nordby, P. O'Connor, M. Oguri, J. Oliver, S.S. Olivier, J.K. Olsen, K. Olsen, E.W. Olszewski, H. Oluseyi, N.D. Padilla, A. Parker, J. Pepper, J.R. Peterson, C. Petry, P.A. Pinto, J.L. Pizagno, B. Popescu, A. Prsa, V. Radcka,

- M.J. Raddick, A. Rasmussen, A. Rau, J. Rho, J.E. Rhoads, G.T. Richards, S.T. Ridgway, B.E. Robertson, R. Roskar, A. Saha, A. Sarajedini, E. Scannapieco, T. Schalk, R. Schindler, S. Schmidt, S. Schmidt, D.P. Schneider, G. Schumacher, R. Scranton, J. Sebag, L.G. Seppala, O. Shemmer, J.D. Simon, M. Sivertz, H.A. Smith, J. Allyn Smith, N. Smith, A.H. Spitz, A. Stanford, K.G. Stassun, J. Strader, M.A. Strauss, C.W. Stubbs, D.W. Sweeney, A. Szalay, P. Szkody, M. Takada, P. Thorman, D.E. Trilling, V. Trimble, A. Tyson, R. Van Berg, D. Vanden Berk, J. VanderPlas, L. Verde, B. Vrsnak, L.M. Walkowicz, B.D. Wandelt, S. Wang, Y. Wang, M. Warner, R.H. Wechsler, A.A. West, O. Wiecha, B.F. Williams, B. Willman, D. Wittman, S.C. Wolff, W.M. Wood-Vasey, P. Wozniak, P. Young, A. Zentner, H. Zhan, LSST Science Book, Version 2.0. arXiv e-prints, 0912-0201 (2009)
- P. Lundqvist, A. Nyholm, F. Taddia, J. Sollerman, J. Johansson, C. Kozma, N. Lundqvist, C. Fransson, P.M. Garnavich, M. Kromer, B.J. Shappee, A. Goobar, No trace of a single-degenerate companion in late spectra of supernovae 2011fe and 2014J. *Astron. Astrophys.* **577**, 39 (2015). doi:10.1051/0004-6361/201525719
- D. Maoz, F. Mannucci, G. Nelemans, Observational Clues to the Progenitors of Type Ia Supernovae. *Annual Review of Astronomy and Astrophysics* **52**, 107–170 (2014). doi:10.1146/annurev-astro-082812-141031
- P.J. Marshall, A. Verma, A. More, C.P. Davis, S. More, A. Kapadia, M. Parrish, C. Snyder, J. Wilcox, E. Baeten, C. Macmillan, C. Cornen, M. Baumer, E. Simpson, C.J. Lintott, D. Miller, E. Paget, R. Simpson, A.M. Smith, R. Küng, P. Saha, T.E. Collett, SPACE WARPS - I. Crowdsourcing the discovery of gravitational lenses. *Mon. Notices of the Royal Astron. Soc.* **455**(2), 1171–1190 (2016). doi:10.1093/mnras/stv2009
- T. Matheson, C. Stubens, N. Wolf, C.-H. Lee, G. Narayan, A. Saha, A. Scott, M. Soraisam, A.S. Bolton, B. Hauger, D.R. Silva, J. Kececioglu, C. Scheidegger, R. Snodgrass, P.D. Aleo, E. Evans-Jacquez, N. Singh, Z. Wang, S. Yang, Z. Zhao, The ANTARES Astronomical Time-domain Event Broker. *Astron. J.* **161**(3), 107 (2021). doi:10.3847/1538-3881/abd703
- R.B. Metcalf, M. Meneghetti, C. Avestruz, F. Bellagamba, C.R. Bom, E. Bertin, R. Cabanac, F. Courbin, A. Davies, E. Decenciére, R. Flamary, R. Gavazzi, M. Geiger, P. Hartley, M. Huertas-Company, N. Jackson, C. Jacobs, E. Jullo, J.-P. Kneib, L.V.E. Koopmans, F. Lanusse, C.-L. Li, Q. Ma, M. Makler, N. Li, M. Lightman, C.E. Petrillo, S. Serjeant, C. Schäfer, A. Sonnenfeld, A. Tagore, C. Tortora, D. Tuccillo, M.B. Valentín, S. Velasco-Forero, G.A. Verdoes Kleijn, G. Vernardos, The strong gravitational lens finding challenge. *Astron. Astrophys.* **625**, 119 (2019). doi:10.1051/0004-6361/201832797
- A.A. Miller, Y. Yao, M. Bulla, C. Pankow, E.C. Bellm, S.B. Cenko, R. Dekany, C. Fremling, M.J. Graham, T. Kupfer, R.R. Laher, A.A. Mahabal, F.J. Masci, P.E. Nugent, R. Riddle, B. Rusholme, R.M. Smith, D.L. Shupe, J. van Roestel, S.R. Kulkarni, ZTF Early Observations of Type Ia Supernovae II: First Light, the Initial Rise, and Time to Reach Maximum Brightness. arXiv e-prints, 2001-00598 (2020)
- M. Millon, F. Courbin, V. Bonvin, E. Paic, G. Meylan, M. Tewes, D. Sluse, P. Magain, J.H.H. Chan, A. Galan, R. Joseph, C. Lemon, O. Tihhonova, R.I. Anderson, M. Marmier, B. Chazelas, M. Lendl, A.H.M.J. Triaud, A. Wyttenbach, COSMOGRAIL. XIX. Time delays in 18 strongly lensed quasars from 15 years

- of optical monitoring. *Astron. Astrophys.* **640**, 105 (2020a). doi:10.1051/0004-6361/202037740
- M. Millon, F. Courbin, V. Bonvin, E. Buckley-Geer, C.D. Fassnacht, J. Frieman, P.J. Marshall, S.H. Suyu, T. Treu, T. Anguita, V. Motta, A. Agnello, J.H.H. Chan, D.C.-Y. Chao, M. Chijani, D. Gilman, K. Gilmore, C. Lemon, J.R. Lucey, A. Melo, E. Paic, K. Rojas, D. Sluse, P.R. Williams, A. Hempel, S. Kim, R. Lachaume, M. Rabus, TDCOSMO. II. Six new time delays in lensed quasars from high-cadence monitoring at the MPIA 2.2 m telescope. *Astron. Astrophys.* **642**, 193 (2020b). doi:10.1051/0004-6361/202038698
- M. Millon, M. Tewes, V. Bonvin, B. Lengen, F. Courbin, PyCS3: A Python toolbox for time-delay measurements in lensed quasars. *The Journal of Open Source Software* **5**(53), 2654 (2020c). doi:10.21105/joss.02654
- A. More, A. Verma, P.J. Marshall, S. More, E. Baeten, J. Wilcox, C. Macmillan, C. Cornen, A. Kapadia, M. Parrish, C. Snyder, C.P. Davis, R. Gavazzi, C.J. Lintott, R. Simpson, D. Miller, A.M. Smith, E. Paget, P. Saha, R. Küng, T.E. Collett, SPACE WARPS- II. New gravitational lens candidates from the CFHTLS discovered through citizen science. *Mon. Notices of the Royal Astron. Soc.* **455**(2), 1191–1210 (2016). doi:10.1093/mnras/stv1965
- A. More, S.H. Suyu, M. Oguri, S. More, C.-H. Lee, Interpreting the Strongly Lensed Supernova iPTF16geu: Time Delay Predictions, Microlensing, and Lensing Rates. *Astrophys. J. Letters* **835**(2), 25 (2017). doi:10.3847/2041-8213/835/2/L25
- M.J. Mortonson, P.L. Schechter, J. Wambsganss, Size Is Everything: Universal Features of Quasar Microlensing with Extended Sources. *Astrophys. J.* **628**(2), 594–603 (2005). doi:10.1086/431195
- E. Mörtsell, J. Johansson, S. Dhawan, A. Goobar, R. Amanullah, D.A. Goldstein, Lens modelling of the strongly lensed Type Ia supernova iPTF16geu. *Mon. Notices of the Royal Astron. Soc.* **496**(3), 3270–3280 (2020). doi:10.1093/mnras/staa1600
- G. Narayan, T. Zaidi, M.D. Soraismam, Z. Wang, M. Lochner, T. Matheson, A. Saha, S. Yang, Z. Zhao, J. Kececioglu, C. Scheidegger, R.T. Snodgrass, T. Axelrod, T. Jenness, R.S. Maier, S.T. Ridgway, R.L. Seaman, E.M. Evans, N. Singh, C. Taylor, J. Toeniskoetter, E. Welch, S. Zhu, ANTARES Collaboration, Machine-learning-based Brokers for Real-time Classification of the LSST Alert Stream. *Astrophys. J. Supplement* **236**(1), 9 (2018). doi:10.3847/1538-4365/aab781
- A.B. Newman, S. Belli, R.S. Ellis, S.G. Patel, Resolving Quiescent Galaxies at $z \gtrsim 2$. I. Search for Gravitationally Lensed Sources and Characterization of Their Structure, Stellar Populations, and Line Emission. *Astrophys. J.* **862**(2), 125 (2018). doi:10.3847/1538-4357/aacd4d
- U.M. Noebauer, M. Kromer, S. Taubenberger, P. Baklanov, S. Blinnikov, E. Sorokina, W. Hillebrandt, Early light curves for Type Ia supernova explosion models. *Mon. Notices of the Royal Astron. Soc.* **472**(3), 2787–2799 (2017). doi:10.1093/mnras/stx2093
- J. Nordin, V. Brinnel, J. van Santen, M. Bulla, U. Feindt, A. Franckowiak, C. Fremling, A. Gal-Yam, M. Giomi, M. Kowalski, A. Mahabal, N. Miranda, L. Rauch, S. Reusch, M. Rigault, S. Schulze, J. Sollerman, R. Stein, O. Yaron, S. van Velzen, C. Ward, Transient processing and analysis using AMPEL: alert management, photometry, and evaluation of light curves. *Astron. Astrophys.* **631**, 147 (2019). doi:10.1051/0004-6361/201935634

- P.E. Nugent, M. Sullivan, S.B. Cenko, R.C. Thomas, D. Kasen, D.A. Howell, D. Bersier, J.S. Bloom, S.R. Kulkarni, M.T. Kandrashoff, A.V. Filippenko, J.M. Silverman, G.W. Marcy, A.W. Howard, H.T. Isaacson, K. Maguire, N. Suzuki, J.E. Tarlton, Y.-C. Pan, L. Bildsten, B.J. Fulton, J.T. Parrent, D. Sand, P. Podsiadlowski, F.B. Bianco, B. Dilday, M.L. Graham, J. Lyman, P. James, M.M. Kasliwal, N.M. Law, R.M. Quimby, I.M. Hook, E.S. Walker, P. Mazzali, E. Pian, E.O. Ofek, A. Gal-Yam, D. Poznanski, Supernova SN 2011fe from an exploding carbon-oxygen white dwarf star. *Nature* **480**(7377), 344–347 (2011). doi:10.1038/nature10644
- M. Oguri, Strong gravitational lensing of explosive transients. *Reports on Progress in Physics* **82**(12), 126901 (2019). doi:10.1088/1361-6633/ab4fc5
- M. Oguri, P.J. Marshall, Gravitationally lensed quasars and supernovae in future wide-field optical imaging surveys. *Mon. Notices of the Royal Astron. Soc.* **405**(4), 2579–2593 (2010). doi:10.1111/j.1365-2966.2010.16639.x
- L. Østman, A. Goobar, E. Mörtsell, Extinction properties of lensing galaxies. *Astron. Astrophys.* **485**(2), 403–415 (2008). doi:10.1051/0004-6361:20079187
- D. Paraficz, J. Hjorth, Gravitational lenses as cosmic rulers: Ω_m , Ω_Λ from time delays and velocity dispersions. *Astron. Astrophys.* **507**(3), 49–52 (2009). doi:10.1051/0004-6361/200913307
- S. Perlmutter, G. Aldering, G. Goldhaber, R.A. Knop, P. Nugent, P.G. Castro, S. Deustua, S. Fabbro, A. Goobar, D.E. Groom, I.M. Hook, A.G. Kim, M.Y. Kim, J.C. Lee, N.J. Nunes, R. Pain, C.R. Pennypacker, R. Quimby, C. Lidman, R.S. Ellis, M. Irwin, R.G. McMahon, P. Ruiz-Lapuente, N. Walton, B. Schaefer, B.J. Boyle, A.V. Filippenko, T. Matheson, A.S. Fruchter, N. Panagia, H.J.M. Newberg, W.J. Couch, T.S.C. Project, Measurements of Ω and Λ from 42 High-Redshift Supernovae. *Astrophys. J.* **517**(2), 565–586 (1999). doi:10.1086/307221
- C.E. Petrillo, C. Tortora, G. Vernerados, L.V.E. Koopmans, G. Verdoes Kleijn, M. Bilicki, N.R. Napolitano, S. Chatterjee, G. Covone, A. Dvornik, T. Erben, F. Getman, B. Giblin, C. Heymans, J.T.A. de Jong, K. Kuijken, P. Schneider, H. Shan, C. Spinelli, A.H. Wright, LinKS: discovering galaxy-scale strong lenses in the Kilo-Degree Survey using convolutional neural networks. *Mon. Notices of the Royal Astron. Soc.* **484**(3), 3879–3896 (2019). doi:10.1093/mnras/stz189
- T. Petrushevska, R. Amanullah, A. Goobar, S. Fabbro, J. Johansson, T. Kjellsson, C. Lidman, K. Paech, J. Richard, H. Dahle, R. Ferretti, J.P. Kneib, M. Limousin, J. Nordin, V. Stanishev, High-redshift supernova rates measured with the gravitational telescope A 1689. *Astron. Astrophys.* **594**, 54 (2016). doi:10.1051/0004-6361/201628925
- T. Petrushevska, R. Amanullah, M. Bulla, M. Kromer, R. Ferretti, A. Goobar, S. Papagiannakis, Testing for redshift evolution of Type Ia supernovae using the strongly lensed PS1-10afx at $z = 1.4$. *Astron. Astrophys.* **603**, 136 (2017). doi:10.1051/0004-6361/201730989
- J.D.R. Pierel, S. Rodney, Turning Gravitationally Lensed Supernovae into Cosmological Probes. *Astrophys. J.* **876**(2), 107 (2019). doi:10.3847/1538-4357/ab164a
- J.D.R. Pierel, S. Rodney, G. Vernerados, M. Oguri, R. Kessler, T. Anguita, Projected Cosmological Constraints from Strongly Lensed Supernovae with the Roman Space Telescope. *Astrophys. J.* **908**(2), 190 (2021). doi:10.3847/1538-4357/abd8d3
- J.D.R. Pierel, N. Arendse, S. Ertl, X. Huang, L.A. Moustakas, S. Schuldt, A.J. Shajib, Y. Shu, S. Birrer, M. Bronikowski, J. Hjorth, S.H. Suyu, S. Agarwal, A.

- Agnello, A.S. Bolton, S. Chakrabarti, C. Cold, F. Courbin, J.M. Della Costa, S. Dhawan, M. Engesser, O.D. Fox, C. Gall, S. Gomez, A. Goobar, C. Jimenez, J. Johansson, G. Li, R. Marques-Chaves, S. Mao, P.A. Mazzali, I. Perez-Fournon, T. Petrushevska, F. Poidevin, A. Rest, W. Sheu, R. Shirley, E. Silver, C. Storfer, T. Treu, R. Wojtak, Y. Zenati, LensWatch: I. Resolved HST Observations and Constraints on the Strongly-Lensed Type Ia Supernova 2022qmx (“SN Zwicky”). arXiv e-prints, 2211–03772 (2022)
- A.L. Piro, V.S. Morozova, Exploring the Potential Diversity of Early Type Ia Supernova Light Curves. *Astrophys. J.* **826**(1), 96 (2016). doi:10.3847/0004-637X/826/1/96
- A.L. Piro, E. Nakar, Constraints on Shallow ^{56}Ni from the Early Light Curves of Type Ia Supernovae. *Astrophys. J.* **784**(1), 85 (2014). doi:10.1088/0004-637X/784/1/85
- A.L. Piro, P. Chang, N.N. Weinberg, Shock Breakout from Type Ia Supernova. *Astrophys. J.* **708**(1), 598–604 (2010). doi:10.1088/0004-637X/708/1/598
- Planck Collaboration, N. Aghanim, Y. Akrami, M. Ashdown, J. Aumont, C. Bacigalupi, M. Ballardini, A.J. Banday, R.B. Barreiro, N. Bartolo, S. Basak, R. Battye, K. Benabed, J.-P. Bernard, M. Bersanelli, P. Bielewicz, J.J. Bock, J.R. Bond, J. Borrill, F.R. Bouchet, F. Boulanger, M. Bucher, C. Burigana, R.C. Butler, E. Calabrese, J.-F. Cardoso, J. Carron, A. Challinor, H.C. Chiang, J. Chluba, L.P.L. Colombo, C. Combet, D. Contreras, B.P. Crill, F. Cuttaia, P. de Bernardis, G. de Zotti, J. Delabrouille, J.-M. Delouis, E. Di Valentino, J.M. Diego, O. Doré, M. Douspis, A. Ducout, X. Dupac, S. Dusini, G. Efstathiou, F. Elsner, T.A. Enßlin, H.K. Eriksen, Y. Fantaye, M. Farhang, J. Ferugsson, R. Fernandez-Cobos, F. Finelli, F. Forastieri, M. Frailis, A.A. Fraisse, E. Franceschi, A. Frolov, S. Galeotta, S. Galli, K. Ganga, R.T. Génova-Santos, M. Gerbino, T. Ghosh, J. González-Nuevo, K.M. Górski, S. Gratton, A. Gruppuso, J.E. Gudmundsson, J. Hamann, W. Handley, F.K. Hansen, D. Herranz, S.R. Hildebrandt, E. Hivon, Z. Huang, A.H. Jaffe, W.C. Jones, A. Karakci, E. Keihänen, R. Keskitalo, K. Kiiveri, J. Kim, T.S. Kisner, L. Knox, N. Krachmalnicoff, M. Kunz, H. Kurki-Suonio, G. Lagache, J.-M. Lamarre, A. Lasenby, M. Lattanzi, C.R. Lawrence, M. Le Jeune, P. Lemos, J. Lesgourgues, F. Levrier, A. Lewis, M. Liguori, P.B. Lilje, M. Lilley, V. Lindholm, M. López-Caniego, P.M. Lubin, Y.-Z. Ma, J.F. Macías-Pérez, G. Maggio, D. Maino, N. Mandolesi, A. Mangilli, A. Marcos-Caballero, M. Maris, P.G. Martin, M. Martinelli, E. Martínez-González, S. Matarrese, N. Mauri, J.D. McEwen, P.R. Meinholt, A. Melchiorri, A. Menella, M. Migliaccio, M. Millea, S. Mitra, M.-A. Miville-Deschénes, D. Molinari, L. Montier, G. Morgante, A. Moss, P. Natoli, H.U. Nørgaard-Nielsen, L. Pagano, D. Paoletti, B. Partridge, G. Patanchon, H.V. Peiris, F. Perrotta, V. Pettorino, F. Piacentini, L. Polastri, G. Polenta, J.-L. Puget, J.P. Rachen, M. Reinecke, M. Remazeilles, A. Renzi, G. Rocha, C. Rosset, G. Roudier, J.A. Rubiño-Martín, B. Ruiz-Granados, L. Salvati, M. Sandri, M. Savelainen, D. Scott, E.P.S. Shellard, C. Sirignano, G. Sirri, L.D. Spencer, R. Sunyaev, A.-S. Suur-Uski, J.A. Tauber, D. Tavagnacco, M. Tenti, L. Toffolatti, M. Tomasi, T. Trombetti, L. Valenziano, J. Valiviita, B. Van Tent, L. Vibert, P. Vielva, F. Villa, N. Vittorio, B.D. Wandelt, I.K. Wehus, M. White, S.D.M. White, A. Zacchei, A. Zonca, Planck 2018 results. VI. Cosmological parameters. *Astron. Astrophys.* **641**, 6 (2020). doi:10.1051/0004-6361/201833910
- R.M. Quimby, M.C. Werner, M. Oguri, S. More, A. More, M. Tanaka, K. Nomoto,

- T.J. Moriya, G. Folatelli, K. Maeda, M. Bersten, Extraordinary Magnification of the Ordinary Type Ia Supernova PS1-10afx. *Astrophys. J. Letters* **768**(1), 20 (2013). doi:10.1088/2041-8205/768/1/L20
- R.M. Quimby, M. Oguri, A. More, S. More, T.J. Moriya, M.C. Werner, M. Tanaka, G. Folatelli, M.C. Bersten, K. Maeda, K. Nomoto, Detection of the Gravitational Lens Magnifying a Type Ia Supernova. *Science* **344**(6182), 396–399 (2014). doi:10.1126/science.1250903
- I. Rabinak, E. Waxman, The Early UV/Optical Emission from Core-collapse Supernovae. *Astrophys. J.* **728**(1), 63 (2011). doi:10.1088/0004-637X/728/1/63
- S. Refsdal, On the possibility of determining Hubble's parameter and the masses of galaxies from the gravitational lens effect. *Mon. Notices of the Royal Astron. Soc.* **128**, 307 (1964). doi:10.1093/mnras/128.4.307
- A.G. Riess, A.V. Filippenko, P. Challis, A. Clocchiatti, A. Diercks, P.M. Garnavich, R.L. Gilliland, C.J. Hogan, S. Jha, R.P. Kirshner, B. Leibundgut, M.M. Phillips, D. Reiss, B.P. Schmidt, R.A. Schommer, R.C. Smith, J. Spyromilio, C. Stubbs, N.B. Suntzeff, J. Tonry, Observational Evidence from Supernovae for an Accelerating Universe and a Cosmological Constant. *Astron. J.* **116**(3), 1009–1038 (1998). doi:10.1086/300499
- A.G. Riess, S. Casertano, W. Yuan, L.M. Macri, D. Scolnic, Large Magellanic Cloud Cepheid Standards Provide a 1% Foundation for the Determination of the Hubble Constant and Stronger Evidence for Physics beyond Λ CDM. *Astrophys. J.* **876**(1), 85 (2019). doi:10.3847/1538-4357/ab1422
- S.A. Rodney, L.-G. Strolger, P.L. Kelly, M. Bradač, G. Brammer, A.V. Filippenko, R.J. Foley, O. Graur, J. Hjorth, S.W. Jha, C. McCully, A. Molino, A.G. Riess, K.B. Schmidt, J. Selsing, K. Sharon, T. Treu, B.J. Weiner, A. Zitrin, SN Refsdal: Photometry and Time Delay Measurements of the First Einstein Cross Supernova. *Astrophys. J.* **820**(1), 50 (2016). doi:10.3847/0004-637X/820/1/50
- S.A. Rodney, A.G. Riess, T. Dahlen, L.-G. Strolger, H.C. Ferguson, J. Hjorth, T.F. Frederiksen, B.J. Weiner, B. Mobasher, S. Casertano, D.O. Jones, P. Challis, S.M. Faber, A.V. Filippenko, P. Garnavich, O. Graur, N.A. Grogin, B. Hayden, S.W. Jha, R.P. Kirshner, D. Kocevski, A. Koekemoer, C. McCully, B. Patel, A. Rajan, C. Scarlata, A Type Ia Supernova at Redshift 1.55 in Hubble Space Telescope Infrared Observations from CANDELS. *Astrophys. J.* **746**(1), 5 (2012). doi:10.1088/0004-637X/746/1/5
- S.A. Rodney, G.B. Brammer, J.D.R. Pierel, J. Richard, S. Toft, K.F. O'Connor, M. Akhshik, K. Whitaker, A Gravitationally Lensed Supernova with an Observable Two-Decade Time Delay. arXiv e-prints, 2106–08935 (2021)
- K. Rojas, E. Savary, B. Clément, M. Maus, F. Courbin, C. Lemon, J.H.H. Chan, G. Vernardos, R. Joseph, R. Cañameras, A. Galan, Search of strong lens systems in the Dark Energy Survey using convolutional neural networks. *Astron. Astrophys.* **668**, 73 (2022). doi:10.1051/0004-6361/202142119
- F.K. Röpke, M. Kromer, I.R. Seitenzahl, R. Pakmor, S.A. Sim, S. Taubenberger, F. Ciaraldi-Schoolmann, W. Hillebrandt, G. Aldering, P. Antilogus, C. Baltay, S. Benitez-Herrera, S. Bongard, C. Buton, A. Canto, F. Cellier-Holzem, M. Childress, N. Chotard, Y. Copin, H.K. Fakhouri, M. Fink, D. Fouchez, E. Gangler, J. Guy, S. Hachinger, E.Y. Hsiao, J. Chen, M. Kerschhaggl, M. Kowalski, P. Nugent, K. Paech, R. Pain, E. Pecontal, R. Pereira, S. Perlmutter, D. Rubinowitz, M. Rigault, K. Runge, C. Saunders, G. Smadja, N. Suzuki, C. Tao, R.C. Thomas, A. Tilquin, C. Wu, Constraining Type Ia Supernova Models: SN

- 2011fe as a Test Case. *Astrophys. J. Letters* **750**(1), 19 (2012). doi:10.1088/2041-8205/750/1/L19
- A. Saha, T. Matheson, R. Snodgrass, J. Kececioglu, G. Narayan, R. Seaman, T. Jenness, T. Axelrod, ANTARES: a prototype transient broker system, in *Observatory Operations: Strategies, Processes, and Systems V*, ed. by A.B. Peck, C.R. Benn, R.L. Seaman Society of Photo-Optical Instrumentation Engineers (SPIE) Conference Series, vol. 9149, 2014, p. 914908. doi:10.1117/12.2056988
- E. Savary, K. Rojas, M. Maus, B. Clément, F. Courbin, R. Gavazzi, J.H.H. Chan, C. Lemon, G. Vernardos, R. Cañameras, S. Schuldt, S.H. Suyu, J.-C. Cuillandre, S. Fabbro, S. Gwyn, M.J. Hudson, M. Kilbinger, D. Scott, C. Stone, Strong lensing in UNIONS: Toward a pipeline from discovery to modeling. *Astron. Astrophys.* **666**, 1 (2022). doi:10.1051/0004-6361/202142505
- P.L. Schechter, J. Wambsganss, Quasar Microlensing at High Magnification and the Role of Dark Matter: Enhanced Fluctuations and Suppressed Saddle Points. *Astrophys. J.* **580**(2), 685–695 (2002). doi:10.1086/343856
- E.F. Schlafly, J.E.G. Peek, D.P. Finkbeiner, G.M. Green, Mapping the extinction curve in 3d: Structure on kiloparsec scales. *The Astrophysical Journal* **838**(1), 36 (2017). doi:10.3847/1538-4357/aa619d. <https://doi.org/10.3847/1538-4357/aa619d>
- P. Schneider, Can one determine cosmological parameters from multi-plane strong lens systems? *Astron. Astrophys.* **568**, 2 (2014). doi:10.1051/0004-6361/201424450
- P. Schneider, D. Sluse, Source-position transformation: an approximate invariance in strong gravitational lensing. *Astron. Astrophys.* **564**, 103 (2014). doi:10.1051/0004-6361/201322106
- D.M. Scolnic, D.O. Jones, A. Rest, Y.C. Pan, R. Chornock, R.J. Foley, M.E. Huber, R. Kessler, G. Narayan, A.G. Riess, S. Rodney, E. Berger, D.J. Brout, P.J. Challis, M. Drout, D. Finkbeiner, R. Lunnan, R.P. Kirshner, N.E. Sanders, E. Schlafly, S. Smartt, C.W. Stubbs, J. Tonry, W.M. Wood-Vasey, M. Foley, J. Hand, E. Johnson, W.S. Burgett, K.C. Chambers, P.W. Draper, K.W. Hodapp, N. Kaiser, R.P. Kudritzki, E.A. Magnier, N. Metcalfe, F. Bresolin, E. Gall, R. Kotak, M. McCrum, K.W. Smith, The Complete Light-curve Sample of Spectroscopically Confirmed SNe Ia from Pan-STARRS1 and Cosmological Constraints from the Combined Pantheon Sample. *Astrophys. J.* **859**(2), 101 (2018). doi:10.3847/1538-4357/aab9bb
- A.J. Shajib, S. Birrer, T. Treu, M.W. Auger, A. Agnello, T. Anguita, E.J. Buckley-Geer, J.H.H. Chan, T.E. Collett, F. Courbin, C.D. Fassnacht, J. Frieman, I. Kayo, C. Lemon, H. Lin, P.J. Marshall, R. McMahon, A. More, N.D. Morgan, V. Motta, M. Oguri, F. Ostrovski, C.E. Rusu, P.L. Schechter, T. Shanks, S.H. Suyu, G. Meylan, T.M.C. Abbott, S. Allam, J. Annis, S. Avila, E. Bertin, D. Brooks, A. Carnero Rosell, M. Carrasco Kind, J. Carretero, C.E. Cunha, L.N. da Costa, J. De Vicente, S. Desai, P. Doel, B. Flaugher, P. Fosalba, J. García-Bellido, D.W. Gerdes, D. Gruen, R.A. Gruendl, G. Gutierrez, W.G. Hartley, D.L. Hollowood, B. Hoyle, D.J. James, K. Kuehn, N. Kuropatkin, O. Lahav, M. Lima, M.A.G. Maia, M. March, J.L. Marshall, P. Melchior, F. Menanteau, R. Miquel, A.A. Plazas, E. Sanchez, V. Scarpine, I. Sevilla-Noarbe, M. Smith, M. Soares-Santos, F. Sobreira, E. Suchyta, M.E.C. Swanson, G. Tarle, A.R. Walker, Is every strong lens model unhappy in its own way? Uniform modelling of a sample of 13 quadruply+ imaged quasars. *Mon. Notices of the Royal Astron.*

- Soc. **483**(4), 5649–5671 (2019). doi:10.1093/mnras/sty3397
- A.J. Shajib, P. Mozumdar, G.C.-F. Chen, T. Treu, M. Cappellari, S. Knabel, S.H. Suyu, V.N. Bennert, J.A. Frieman, D. Sluse, S. Birrer, F. Courbin, C.D. Fassnacht, L. Villafañá, P.R. Williams, TDCOSMO. XIII. Improved Hubble constant measurement from lensing time delays using spatially resolved stellar kinematics of the lens galaxy. arXiv e-prints, 2301–02656 (2023)
- A. Sherstinsky, Fundamentals of Recurrent Neural Network (RNN) and Long Short-Term Memory (LSTM) network. Physica D Nonlinear Phenomena **404**, 132306 (2020). doi:10.1016/j.physd.2019.132306
- W. Sheu, X. Huang, A. Cikota, N. Suzuki, D. Schlegel, C. Storfer, Retrospective Search for Strongly Lensed Supernovae in the DESI Legacy Imaging Surveys. arXiv e-prints, 2301–03578 (2023)
- Y. Shu, J.R. Brownstein, A.S. Bolton, L.V.E. Koopmans, T. Treu, A.D. Montero-Dorta, M.W. Auger, O. Czoske, R. Gavazzi, P.J. Marshall, L.A. Moustakas, The Sloan Lens ACS Survey. XIII. Discovery of 40 New Galaxy-scale Strong Lenses. Astrophys. J. **851**(1), 48 (2017). doi:10.3847/1538-4357/aa9794
- Y. Shu, A.S. Bolton, S. Mao, X. Kang, G. Li, M. Soraisam, Prediction of Supernova Rates in Known Galaxy-Galaxy Strong-lens Systems. Astrophys. J. **864**(1), 91 (2018). doi:10.3847/1538-4357/aad5ea
- Y. Shu, R. Cañameras, S. Schuldt, S.H. Suyu, S. Taubenberger, K.T. Inoue, A.T. Jaelani, HOLISMOKES. VIII. High-redshift, strong-lens search in the Hyper Suprime-Cam Subaru Strategic Program. Astron. Astrophys. **662**, 4 (2022). doi:10.1051/0004-6361/202243203
- S.A. Sim, F.K. Röpke, W. Hillebrandt, M. Kromer, R. Pakmor, M. Fink, A.J. Ruiter, I.R. Seitenzahl, Detonations in Sub-Chandrasekhar-mass C+O White Dwarfs. Astrophys. J. Letters **714**(1), 52–57 (2010). doi:10.1088/2041-8205/714/1/L52
- K.W. Smith, R.D. Williams, D.R. Young, A. Ibsen, S.J. Smartt, A. Lawrence, D. Morris, S. Voutsinas, M. Nicholl, Lasair: The Transient Alert Broker for LSST:UK. Research Notes of the American Astronomical Society **3**(1), 26 (2019). doi:10.3847/2515-5172/ab020f
- A. Sonnenfeld, J.H.H. Chan, Y. Shu, A. More, M. Oguri, S.H. Suyu, K.C. Wong, C.-H. Lee, J. Coupon, A. Yonehara, A.S. Bolton, A.T. Jaelani, M. Tanaka, S. Miyazaki, Y. Komiyama, Survey of Gravitationally-lensed Objects in HSC Imaging (SuGOHI). I. Automatic search for galaxy-scale strong lenses. Publ. of the Astron. Soc. of Japan **70**, 29 (2018). doi:10.1093/pasj/psx062
- A. Sonnenfeld, A. Verma, A. More, E. Baeten, C. Macmillan, K.C. Wong, J.H.H. Chan, A.T. Jaelani, C.-H. Lee, M. Oguri, C.E. Rusu, M. Veldthuis, L. Trouille, P.J. Marshall, R. Hutchings, C. Allen, J. O'Donnell, C. Cornen, C.P. Davis, A. McMaster, C. Lintott, G. Miller, Survey of Gravitationally-lensed Objects in HSC Imaging (SuGOHI). VI. Crowdsourced lens finding with Space Warps. Astron. Astrophys. **642**, 148 (2020). doi:10.1051/0004-6361/202038067
- V. Stanishev, A. Goobar, K. Paech, R. Amanullah, T. Dahlén, J. Jönsson, J.P. Kneib, C. Lidman, M. Limousin, E. Mörtsell, S. Nobili, J. Richard, T. Riehm, M. von Strauss, Near-IR search for lensed supernovae behind galaxy clusters. I. Observations and transient detection efficiency. Astron. Astrophys. **507**(1), 61–69 (2009). doi:10.1051/0004-6361/200911982
- M. Sullivan, R. Ellis, P. Nugent, I. Smail, P. Madau, A strategy for finding gravitationally lensed distant supernovae. Mon. Notices of the Royal Astron. Soc.

- 319**(2), 549–556 (2000). doi:10.1046/j.1365-8711.2000.03875.x
- Y. Suwa, Supernova forecast with strong lensing. *Mon. Notices of the Royal Astron. Soc.* **474**(2), 2612–2616 (2018). doi:10.1093/mnras/stx2953
- S.H. Suyu, P.J. Marshall, M.W. Auger, S. Hilbert, R.D. Blandford, L.V.E. Koopmans, C.D. Fassnacht, T. Treu, Dissecting the Gravitational lens B1608+656. II. Precision Measurements of the Hubble Constant, Spatial Curvature, and the Dark Energy Equation of State. *Astrophys. J.* **711**(1), 201–221 (2010). doi:10.1088/0004-637X/711/1/201
- S.H. Suyu, S. Huber, R. Cañameras, M. Kromer, S. Schuldt, S. Taubenberger, A. Yıldırım, V. Bonvin, J.H.H. Chan, F. Courbin, U. Nöbauer, S.A. Sim, D. Sluse, HOLISMOKES. I. Highly Optimised Lensing Investigations of Supernovae, Microlensing Objects, and Kinematics of Ellipticals and Spirals. *Astron. Astrophys.* **644**, 162 (2020). doi:10.1051/0004-6361/202037757
- S.H. Suyu, T.-C. Chang, F. Courbin, T. Okumura, Cosmological Distance Indicators. *Space Science Reviews* **214**(5), 91 (2018). doi:10.1007/s11214-018-0524-3
- M. Tewes, F. Courbin, G. Meylan, COSMOGRAIL: the COSmological MOonitoring of GRAVItational Lenses. XI. Techniques for time delay measurement in presence of microlensing. *Astron. Astrophys.* **553**, 120 (2013). doi:10.1051/0004-6361/201220123
- K.-V.H. Tran, A. Harshan, K. Glazebrook, G.C. Keerthi Vasan, T. Jones, C. Jacobs, G.G. Kacprzak, T.M. Barone, T.E. Collett, A. Gupta, A. Henderson, L.J. Kewley, S. Lopez, T. Nanayakkara, R.L. Sanders, S.M. Sweet, The AGEL Survey: Spectroscopic Confirmation of Strong Gravitational Lenses in the DES and DECaLS Fields Selected Using Convolutional Neural Networks. *Astron. J.* **164**(4), 148 (2022). doi:10.3847/1538-3881/ac7da2
- T. Treu, G. Brammer, J.M. Diego, C. Grillo, P.L. Kelly, M. Oguri, S.A. Rodney, P. Rosati, K. Sharon, A. Zitrin, I. Balestra, M. Bradač, T. Broadhurst, G.B. Caminha, A. Halkola, A. Hoag, M. Ishigaki, T.L. Johnson, W. Karman, R. Kawamata, A. Mercurio, K.B. Schmidt, L.-G. Strolger, S.H. Suyu, A.V. Filippenko, R.J. Foley, S.W. Jha, B. Patel, “Refsdal” Meets Popper: Comparing Predictions of the Re-appearance of the Multiply Imaged Supernova Behind MACSJ1149.5+2223. *Astrophys. J.* **817**(1), 60 (2016). doi:10.3847/0004-637X/817/1/60
- T. Treu, P.J. Marshall, Time delay cosmography. *Astron. Astrophys. Review* **24**(1), 11 (2016). doi:10.1007/s00159-016-0096-8
- T. Treu, S.H. Suyu, P.J. Marshall, Strong lensing time-delay cosmography in the 2020s. *Astron. Astrophys. Review* **30**(1), 8 (2022). doi:10.1007/s00159-022-00145-y
- L. Verde, T. Treu, A.G. Riess, Tensions between the early and late Universe. *Nature Astronomy* **3**, 891–895 (2019). doi:10.1038/s41550-019-0902-0
- G. Vernardos, C.J. Fluke, Adventures in the microlensing cloud: Large datasets, eResearch tools, and GPUs. *Astronomy and Computing* **6**, 1–18 (2014). doi:10.1016/j.ascom.2014.05.002
- G. Vernardos, C.J. Fluke, N.F. Bate, D. Croton, GERLUMPH Data Release 1: High-resolution Cosmological Microlensing Magnification Maps and eResearch Tools. *Astrophys. J. Supplement* **211**(1), 16 (2014). doi:10.1088/0067-0049/211/1/16
- G. Vernardos, C.J. Fluke, N.F. Bate, D. Croton, D. Vohl, GERLUMPH Data Release 2: 2.5 Billion Simulated Microlensing Light Curves. *Astrophys. J. Supplement*

- plement **217**(2), 23 (2015). doi:10.1088/0067-0049/217/2/23
- G. Vernardos, G. Tsagkatakis, Quasar microlensing light-curve analysis using deep machine learning. *Mon. Notices of the Royal Astron. Soc.* **486**(2), 1944–1952 (2019). doi:10.1093/mnras/stz868
- J.D. Vieira, D.P. Marrone, S.C. Chapman, C. De Breuck, Y.D. Hezaveh, A. Weiβ, J.E. Aguirre, K.A. Aird, M. Aravena, M.L.N. Ashby, M. Bayliss, B.A. Benson, A.D. Biggs, L.E. Bleem, J.J. Bock, M. Bothwell, C.M. Bradford, M. Brodwin, J.E. Carlstrom, C.L. Chang, T.M. Crawford, A.T. Crites, T. de Haan, M.A. Dobbs, E.B. Fomalont, C.D. Fassnacht, E.M. George, M.D. Gladders, A.H. Gonzalez, T.R. Greve, B. Gullberg, N.W. Halverson, F.W. High, G.P. Holder, W.L. Holzapfel, S. Hoover, J.D. Hrubes, T.R. Hunter, R. Keisler, A.T. Lee, E.M. Leitch, M. Lueker, D. Luong-van, M. Malkan, V. McIntyre, J.J. McMahon, J. Mehl, K.M. Menten, S.S. Meyer, L.M. Mocanu, E.J. Murphy, T. Natoli, S. Padin, T. Plagge, C.L. Reichardt, A. Rest, J. Ruel, J.E. Ruhl, K. Sharon, K.K. Schaffer, L. Shaw, E. Shirokoff, J.S. Spilker, B. Stalder, Z. Staniszewski, A.A. Stark, K. Story, K. Vanderlinde, N. Welikala, R. Williamson, Dusty starburst galaxies in the early Universe as revealed by gravitational lensing. *Nature* **495**(7441), 344–347 (2013). doi:10.1038/nature12001
- C. Vogl, S.A. Sim, U.M. Noebauer, W.E. Kerzendorf, W. Hillebrandt, Spectral modeling of type II supernovae. I. Dilution factors. *Astron. Astrophys.* **621**, 29 (2019). doi:10.1051/0004-6361/201833701
- C. Vogl, W.E. Kerzendorf, S.A. Sim, U.M. Noebauer, S. Lietzau, W. Hillebrandt, Spectral modeling of type II supernovae. II. A machine-learning approach to quantitative spectroscopic analysis. *Astron. Astrophys.* **633**, 88 (2020). doi:10.1051/0004-6361/201936137
- D. Walsh, R.F. Carswell, R.J. Weymann, 0957+561 A, B: twin quasistellar objects or gravitational lens? *Nature* **279**, 381–384 (1979). doi:10.1038/279381a0
- R.F. Webbbink, Double white dwarfs as progenitors of R Coronae Borealis stars and Type I supernovae. *Astrophys. J.* **277**, 355–360 (1984). doi:10.1086/161701
- L. Weisenbach, P.L. Schechter, S. Pontula, “Worst-case” Microlensing in the Identification and Modeling of Lensed Quasars. *Astrophys. J.* **922**(1), 70 (2021). doi:10.3847/1538-4357/ac2228
- J. Whelan, I. Iben Jr., Binaries and Supernovae of Type I. *Astrophys. J.* **186**, 1007–1014 (1973). doi:10.1086/152565
- R. Wojtak, J. Hjorth, C. Gall, Magnified or multiply imaged? - Search strategies for gravitationally lensed supernovae in wide-field surveys. *Mon. Notices of the Royal Astron. Soc.* **487**(3), 3342–3355 (2019). doi:10.1093/mnras/stz1516
- K.C. Wong, S.H. Suyu, G.C.-F. Chen, C.E. Rusu, M. Millon, D. Sluse, V. Bonvin, C.D. Fassnacht, S. Taubenberger, M.W. Auger, S. Birrer, J.H.H. Chan, F. Courbin, S. Hilbert, O. Tihhonova, T. Treu, A. Agnello, X. Ding, I. Jee, E. Komatsu, A.J. Shajib, A. Sonnenfeld, R.D. Blandford, L.V.E. Koopmans, P.J. Marshall, G. Meylan, H0LiCOW – XIII. A 2.4 per cent measurement of H_0 from lensed quasars: 5.3 σ tension between early- and late-Universe probes. *Mon. Notices of the Royal Astron. Soc.* **498**(1), 1420–1439 (2020). doi:10.1093/mnras/stz3094
- D.A. Yahalom, P.L. Schechter, J. Wambsganss, A Quadruply Lensed SN Ia: Gaining a Time-Delay...Losing a Standard Candle. arXiv e-prints, 1711-07919 (2017)
- Y. Yao, A.A. Miller, S.R. Kulkarni, M. Bulla, F.J. Masci, D.A. Goldstein, A. Goobar, P. Nugent, A. Dugas, N. Blagorodnova, J.D. Neill, M. Rigault, J. Sollerman,

- J. Nordin, E.C. Bellm, S.B. Cenko, K. De, S. Dhawan, U. Feindt, C. Fremling, P. Gatkine, M.J. Graham, M.L. Graham, A.Y.Q. Ho, T. Hung, M.M. Kasliwal, T. Kupfer, R.R. Laher, D.A. Perley, B. Rusholme, D.L. Shupe, M.T. Soumagnac, K. Taggart, R. Walters, L. Yan, ZTF Early Observations of Type Ia Supernovae. I. Properties of the 2018 Sample. *Astrophys. J.* **886**(2), 152 (2019). doi:10.3847/1538-4357/ab4cf5
- A. Yıldırım, S.H. Suyu, G.C.-F. Chen, E. Komatsu, TDCOSMO VIII: Cosmological distance measurements in light of the mass-sheet degeneracy – forecasts from strong lensing and IFU stellar kinematics. arXiv e-prints, 2109–14615 (2021)
- A. Yıldırım, S.H. Suyu, A. Halkola, Time-delay cosmographic forecasts with strong lensing and JWST stellar kinematics. *Mon. Notices of the Royal Astron. Soc.* **493**(4), 4783–4807 (2020). doi:10.1093/mnras/staa498
- F. Zwicky, Nebulae as gravitational lenses. *Phys. Rev.* **51**, 290–290 (1937). doi:10.1103/PhysRev.51.290. <https://link.aps.org/doi/10.1103/PhysRev.51.290>